AD-A192 410 COMPUTER-AIDED STRUCTURAL ENGINEERING (CASE) PROJECT PROCEDURE FOR STATIC (U) ARMY ENGINEER WATERWAYS EXPERIMENT STATION VICKSBURG MS INFOR K M WILL 1/1

UNCLASSIFIED DEC 87 WES/TR/ITL-87-8 F/G 13/3 NL

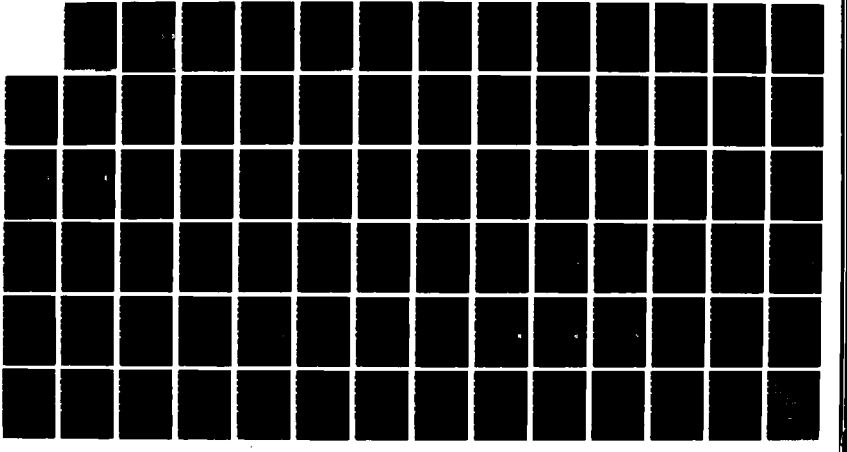


1.0
1.1
1.2
1.4
1.6
1.8
2.0
2.2
2.5
2.8
3.2
3.6
4.0
4.5
5.0
5.6

AD-A192 410

88 3 7

Unclassified
SECURITY CLASSIFICATION OF THIS PAGE

REPORT DOCUMENTATION PAGE

Form Approved
OMB No 0704 0188
Exp Date Jun 30 1986

1a REPORT SECURITY CLASSIFICATION Unclassified	1b RESTRICTIVE MARKINGS
2a SECURITY CLASSIFICATION AUTHORITY	3 DISTRIBUTION / AVAILABILITY OF REPORT Approved for public release; distribution unlimited
2b DECLASSIFICATION / DOWNGRADING SCHEDULE	
4 PERFORMING ORGANIZATION REPORT NUMBER(S) TR-ITL-87-8	5 MONITORING ORGANIZATION REPORT NUMBER(S)
6a NAME OF PERFORMING ORGANIZATION CASE Task Group on Finite Element Analysis 6b OFFICE SYMBOL (If applicable) WESIM-RR	7a NAME OF MONITORING ORGANIZATION US Army Engineer Waterways Experiment Station, Information Technology Laboratory
6c ADDRESS (City, State, and ZIP Code)	7b ADDRESS (City, State, and ZIP Code) PO Box 631 Vicksburg, MS 39180-0631
8a NAME OF FUNDING / SPONSORING ORGANIZATION US Army Corps of Engineers 8b OFFICE SYMBOL (If applicable)	9 PROCUREMENT INSTRUMENT IDENTIFICATION NUMBER
8c ADDRESS (City, State, and ZIP Code) Washington, DC 20314-1000	10 SOURCE OF FUNDING NUMBERS PROGRAM ELEMENT NO / PROJECT NO / TASK NO / WORK UNIT ACCESSION NO

11 TITLE (Include Security Classification)
Procedure for Static Analysis of Gravity Dams Using the Finite Element Method - Phase Ia

12 PERSONAL AUTHOR(S)
Will, Kenneth M. and The CASE Task Group on Finite Element Analysis

13a TYPE OF REPORT	13b TIME COVERED	14 DATE OF REPORT (Year, Month, Day)	15 PAGE COUNT
Final report	FROM _____ TO _____	December 1987	78

16 SUPPLEMENTARY NOTATION
See reverse

17 COSATI CODES			18 SUBJECT TERMS (Continue on reverse if necessary and identify by block number)
FIELD	GROUP	SUB-GROUP	Computer-aided design; Gravity dams; Finite element method; Structural design

19 ABSTRACT (Continue on reverse if necessary and identify by block number)

This study is a continuation of an on-going project by the Computer-Aided Structural Engineering (CASE) Committee on finite element analysis. This method of analysis, though in use for many years, is becoming more widely acclaimed as a viable method of solution available to engineers for structural analyses.

Phase Ia of this study, discussed herein, seeks to inform the engineer of the necessary steps in performing a static finite element analysis of a Corps structure, a gravity dam. Following the preparatory information and the actual analysis, the results are interpreted and the accuracy of the solution is determined. Finally, conclusions and recommendation for finite element modeling of gravity dams are presented.

20 DISTRIBUTION / AVAILABILITY OF ABSTRACT	21 ABSTRACT SECURITY CLASSIFICATION
☒ UNCLASSIFIED UNLIMITED ☐ SAME AS RPT ☐ DTIC USERS	Unclassified
22a NAME OF RESPONSIBLE INDIVIDUAL	22b TELEPHONE (Include Area Code) / 22c OFFICE SYMBOL

DD FORM 1473, 84 MAR — 83 APR edition may be used until exhausted. All other editions are obsolete.

SECURITY CLASSIFICATION OF THIS PAGE
Unclassified

16. SUPPLEMENTARY NOTATION (Continued).

Available from National Technical Information Service, 5285 Port Royal Road, Springfield, VA 22161. This report was prepared under the Computer-Aided Structural Engineering (CASE) Project. A list of CASE reports is printed on the inside of the back cover.

PREFACE

This report is aimed at providing guidance for the use of the finite element method of analysis for the analysis of concrete gravity dams. This Phase Ia report will address only the static analysis of the gravity dam. Phase Ib will address the effect of the foundation in the static analysis of concrete gravity dams. Phase II will address the dynamic analysis of concrete gravity dams. Other future reports will address guidance for other phases of finite element analysis. The work was sponsored under funds provided to the US Army Engineer Waterways Experiment Station (WES) by the Engineering and Construction Directorate, Office, Chief of Engineers (OCE), US Army, as part of the Computer-Aided Structural Engineering (CASE) Project. Mr. Lucian Guthrie, Structures Branch, Engineering and Construction Directorate, was the OCE point of contact.

Input for the report was obtained from the CASE Task Group on Finite Element Analysis. Members and others who directly contributed to the report were:

David Raisanen, North Pacific Division (Chairman)
Barry Fehl, St. Louis District
Dick Huff, Kansas City District
Paul LaHoud, Huntsville Division
Jerry Foster, Federal Energy & Regulatory Commission
Ed Alling, USDA - Soil Conservation Service
Paul Wiersma, Seattle District
Terry West, Jacksonville District
Lucian Guthrie, OCE
N. Radhakrishnan, WES
Robert Hall, WES
H. Wayne Jones, WES
Kenneth Will, Georgia Institute of Technology

The report was compiled and written by Dr. Kenneth M. Will. Engineers from WES, Dr. N. Radhakrishnan, Acting Chief, Information Technology Laboratory (ITL), formerly Automation Technology Center (ATC), and CASE Project Manager, along with Dr. Robert Hall, Research Civil Engineer, Structures Laboratory, formerly associated with ATC, and Mr. H. Wayne Jones, Civil Engineer, ITL, monitored the work. This report was edited by Ms. Gilda Miller, Information Products Division, ITL, WES, with Ms. Deborah Shiers coordinating text and figure layout.

COL Dwayne G. Lee, CE, is the Commander and Director of WES. Dr. Robert W. Whalin is Technical Director.

CONTENTS

CONVERSION FACTORS, NON-SI TO SI (METRIC) UNITS OF MEASUREMENT

Non-SI units of measurement used in this report can be converted to SI (metric) units as follows:

Multiply	By	To Obtain
feet	0.3048	metres
inches	2.54	centimetres
kips (force)	4.448222	kilonewtons
pounds (mass) per cubic foot	16.01846	kilograms per cubic metre
pounds (force) per foot	14.5939	newtons per metre
pounds (force) per inch	175.1268	newtons per metre
pounds (force) per square inch	6.894757	kilopascals

PROCEDURE FOR STATIC ANALYSIS OF GRAVITY DAMS USING THE FINITE ELEMENT METHOD - PHASE Ia

PART I: INTRODUCTION

Finite Element Analysis Study

1. This study has been prepared as part of an on-going effort by the Computer-Aided Structural Engineering (CASE) Committee on finite element analysis. Although the finite element method has been in commercial use since the late 1950's, many engineers are just realizing the benefits of the technique or determining that there is no other method of solution available for many of today's structural analyses and design requirements. With this increased interest in the method, a Corps-wide program has been initiated to provide standardized guidance for the use of the finite element method.

Objectives and Necessary Steps for Finite Element Analysis

2. The primary objective in Phase Ia of this study is to familiarize the engineer with the necessary steps in performing a static finite element analysis of a typical Corps civil works structure, a gravity dam monolith. Many of the steps taken in the analysis of the dam will apply to the analysis of any structure. Therefore, the beginning finite element analyst should develop an understanding of the necessary steps as well as an understanding of the actual analysis of a gravity dam.

3. The necessary steps in performing a finite element analysis are presented below:

a. Select a finite element computer program currently in use by the Corps or in widespread use by private engineering firms and supported by a vendor.

b. Select a simple problem for analysis as close as possible in overall geometry, material properties, boundary conditions, and loading conditions to the real structure. This structure should have closed-form, experimental, or other analytical solution results available.

c. Select the finite element types to be used in the analysis from the library of elements available in the program chosen in step a.

d. Develop and analyze finite element models of the simplified structure and compare results, such as deflections and stresses, with the closed-form results.

e. Develop modeling guidelines from the results of step d, which may be extended to the real structure.

f. Prepare a finite element model of the real structure and perform an analysis.

g. Ask the following question: Is the solution acceptable? If the answer is no, refine and reanalyze until the answer is yes.

4. Before actually performing the analysis, further detailed discussion of these steps is warranted to understand their necessity:

a. In step 3a the key concept is that the finite element program should be currently used by the Corps or other engineering firms and supported by a vendor. There are numerous finite element programs available today, and care must be taken in the selection process. While factors such as ease of use, functional capabilities, and price are extremely important, an overriding consideration is the use of the program within the Corps or other engineering firms and support by the vendor. An ideal situation is to find a program that is easy to use, has the necessary functional capabilities, is reasonably priced, and is currently being used by someone within the engineer's group and is supported by the vendor.

b. The motivation for steps 3a through 3d is to provide an opportunity for the engineer to build confidence in the use of the program and finite element modeling techniques and to develop an understanding of the convergence criteria. Another important reason for these steps is to provide the engineer with an understanding of the type, quantity, and quality of finite element results. A much too common occurrence is for the engineer to devote an enormous amount of time to developing the finite element model. After results have been obtained, too little time is then devoted to the interpretation of these results, i.e., the accuracy of the results or their actual usage in the design process.

c. From the analysis performed in steps 3b through 3d, the engineer must then extrapolate the information gained from the modeling of the simple structure to the modeling of the real structure. Guidelines such as the number of subdivisions of the mesh in the horizontal and vertical directions may be developed for use in the initial model of the real structure.

d. In step 3f, the real structure is modeled and analyzed, and the results are interpreted. This leads to crucial questions in the analysis: Is the solution accurate within an error criteria developed by the engineer? How much error is there? These are the most difficult and crucial questions in the entire process. In many instances, the only correct way to answer these questions is to refine the model, reanalyze, and compare solutions. The following question should then be asked: Have the results

changed significantly due to the refinement? If not, an approximate solution has converged and the engineer must determine whether or not the results make physical sense. If the results have changed significantly, other models may be required and comparisons repeated until convergence is satisfied. The engineer must keep in mind that the finite element method is an approximate solution technique.

Scope

5. In performing the steps in paragraph 3 for the analysis of a gravity dam, this phase of the study is limited to developing a method to analyze the deflections and stresses of the gravity concrete structure only. Interaction between the structure and foundation is not considered at this time. The program selected in step 3a was GTSTRUDL,* since it is well supported and currently is widely used by the Corps. Also, GTSTRUDL is representative of a general-purpose finite element program.

6. Part II of this report presents an example of steps 3b through 3d in preparation for the analysis of a gravity dam. The actual analysis of a nonoverflow mono ith with geometry similar to that of the Richard B. Russell (RBR) Dam is presented in Part III. Conclusions and recommendations for finite element modeling of gravity dams are presented in Part IV.

---

* GTSTRUDL is a general-purpose finite element program owned and maintained by the GTICES Systems Laboratory, School of Civil Engineering, Georgia Institute of Technology. Program runs used in this report were made on the Control Data Corporation, Cybernet Computer System.

PART II: FINITE ELEMENT ANALYSIS OF A SIMPLIFIED STRUCTURE

Selection of a Simplified Structure

7. After selecting a finite element program such as GTSTRUDL, the beginning analyst must then select a simplified model that exhibits as many characteristics (overall geometry, boundary conditions, material properties, and loadings) as possible of the real structure to be analyzed. If possible, a structure should be chosen for which there are other analytical, experimental, or numerical solutions available. Based on these requirements, two simple cantilevered structures with two loading conditions were selected for the analysis. These structures are shown in Figure 1.*

8. The structure in Figure 1a is a rectangular cantilever beam (Case A) with overall dimensions similar to the average dimensions of the real dam monolith structure. Two loading cases were used for the analyses: (1) a concentrated force at the top (Case A1) and (2) a linear varying force over the height (Case A2). The first loading was selected due to its simplicity, while the second loading represents a hydrostatic pressure applied along the vertical centroidal axis over the full height of the structure.

9. The second structure shown in Figure 1b is a trapezoidal cantilever beam (Case B) with the same two loading cases as the rectangular cantilever (Cases B1 and B2). The trapezoidal cantilever more closely approaches the shape of the real gravity dam monolith.

10. Another factor influencing the choice of these structures and loadings was the availability of analytical solutions. Timoshenko Beam Theory** and Theory of Elasticity** solutions were available for both structures and loadings except for the hydrostatic loading on the trapezoidal cantilever.

Selection of Elements

11. Based on the requirements for the gravity dam analysis, five major

---

* A table of factors for converting non-SI units of measurement to SI (metric) units is presented on page 3.

** S. P. Timoshenko and J. N. Goodier. 1951. Theory of Elasticity, McGraw-Hill, New York.

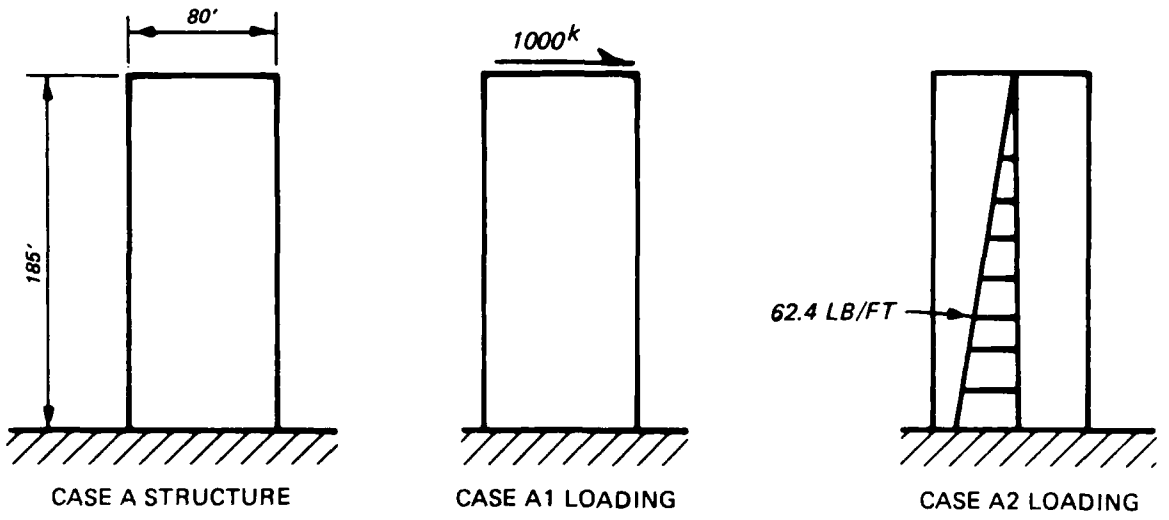

a. Rectangular cantilever--Case A

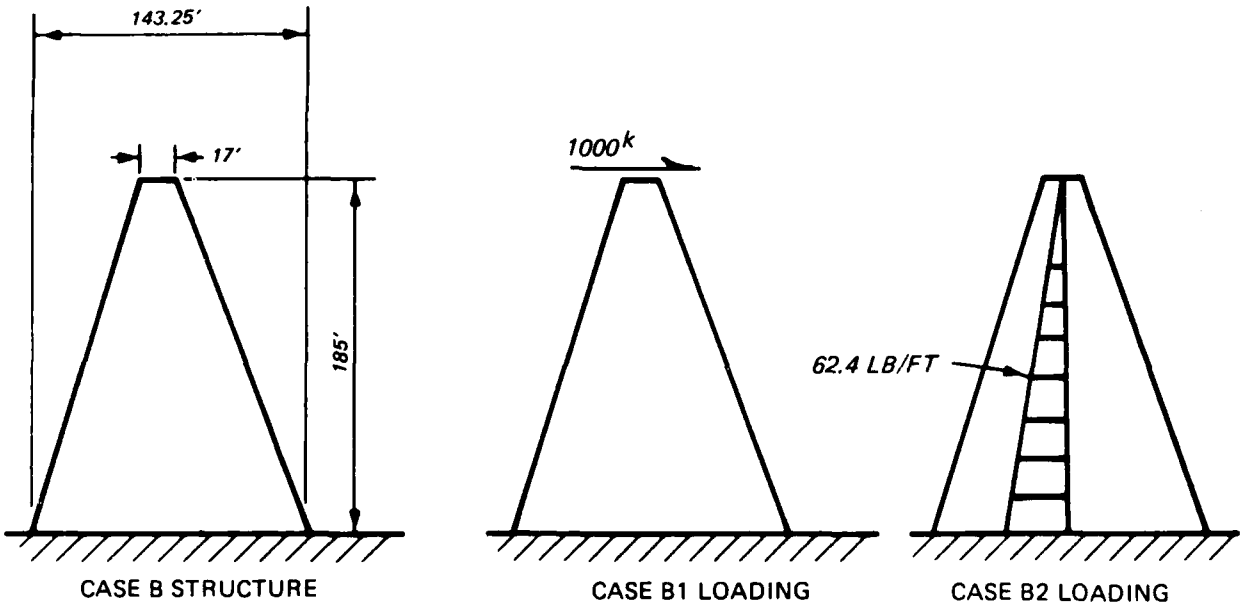

b. Trapezoidal cantilever--Case B

Figure 1. Simplified structure models

points were considered in selecting a plane stress/strain element from the GTSTRUDL element library:

a. The element must represent quadrilateral regions and not be restricted to rectangular shape. Although triangular elements may be combined to represent a quadrilateral, input is increased since at least twice as many elements must now be input. The quantity of output is also increased. Thus, it is desirable to use an element that can represent a quadrilateral region.

b. The element must accommodate edge loads to represent the hydrostatic loading.

c. The element must represent thermal loads. This capability may be used in another phase of this study.

d. The element must represent body forces to account for the self-weight of the structure.

e. The element should be accurate with no undesirable behavior such as incompatibility with adjacent elements. The goal is to find the element that produces the most accurate results for the least cost.

12. After evaluating the GTSTRUDL element library, the IPLQ and IPQQ elements were found to satisfy the requirements in paragraph 11. The IPLQ is a simple quadrilateral element with only four corner nodes, while the IPQQ quadrilateral element has eight nodes and allows for curved edges. Since curved edges were not required in the dam monolith, the final selection was based on the most accurate element for the least cost. Both elements are fully compatible with adjacent elements and belong to the well-known isoparametric family of elements. Generally, the IPQQ element has produced slightly more accurate answers for the least total cost, since more IPLQ elements are needed to produce an equivalent solution. Therefore, the IPQQ element was selected for use in the analysis of the simplified structures as well as the actual dam monolith.

Finite Element Models of Simplified Structures

Finite element meshes

13. Three different models were developed for the cantilevers to ensure convergence to the correct solution. The various models are called the coarse, fine, and very fine meshes to indicate the relative degree of refinement. They are also called meshes 1, 2, and 3 with mesh 1 having the fewest number of elements and mesh 3 having the most elements. These meshes for the

rectangular cantilever are illustrated in Figures 2 through 4 with nodes and elements labeled in each figure. A summary of the meshes is presented below:

	No. of Nodes	No. of IPQQ Elements
Mesh 1	45	10
Mesh 2	149	40
Mesh 3	537	160

14. After analyzing the rectangular cantilever with all three meshes, the decision was made to use meshes 1 and 2 only for the trapezoidal cantilever as discussed in paragraph 29. Meshes 1 and 2 for the trapezoidal cantilever are presented in Figures 5 and 6. For both the rectangular and trapezoidal models, equal subdivisions of the meshes in the horizontal and vertical directions were used. In particular, this simplified the automatic generation of the meshes.

Loadings

15. Two loading conditions were considered for each structure, the horizontal force at the top of the cantilevers and the linear varying load over the height which represented a hydrostatic loading. For the concentrated loading condition, the force was distributed to all the nodes at the top using a tributary area concept. Ideally, if the cantilevers were behaving according to beam theory, a parabolic distribution of the concentrated load should be imposed since the shear stress distribution is also parabolic. However, the shear stress distribution for the trapezoidal cantilever is not the same as from beam theory and the tributary area concept was chosen due to its simplicity. Either technique should produce the same results as the distance from the point of application of the loading increases. The hydrostatic loading condition was modeled using edge loads along one edge of the elements on the right of the centroidal axis. The loading was applied on the centroidal axis to match beam theory results as closely as possible.

Boundary conditions

16. The boundary conditions at the base of the cantilever were the same for the rectangular and trapezoidal cantilevers. For both cases, the node on the centroidal axis was completely restrained while the other nodes along the base were on rollers which permitted horizontal motion. While these boundary conditions do not represent a true fixed condition, they do agree as closely

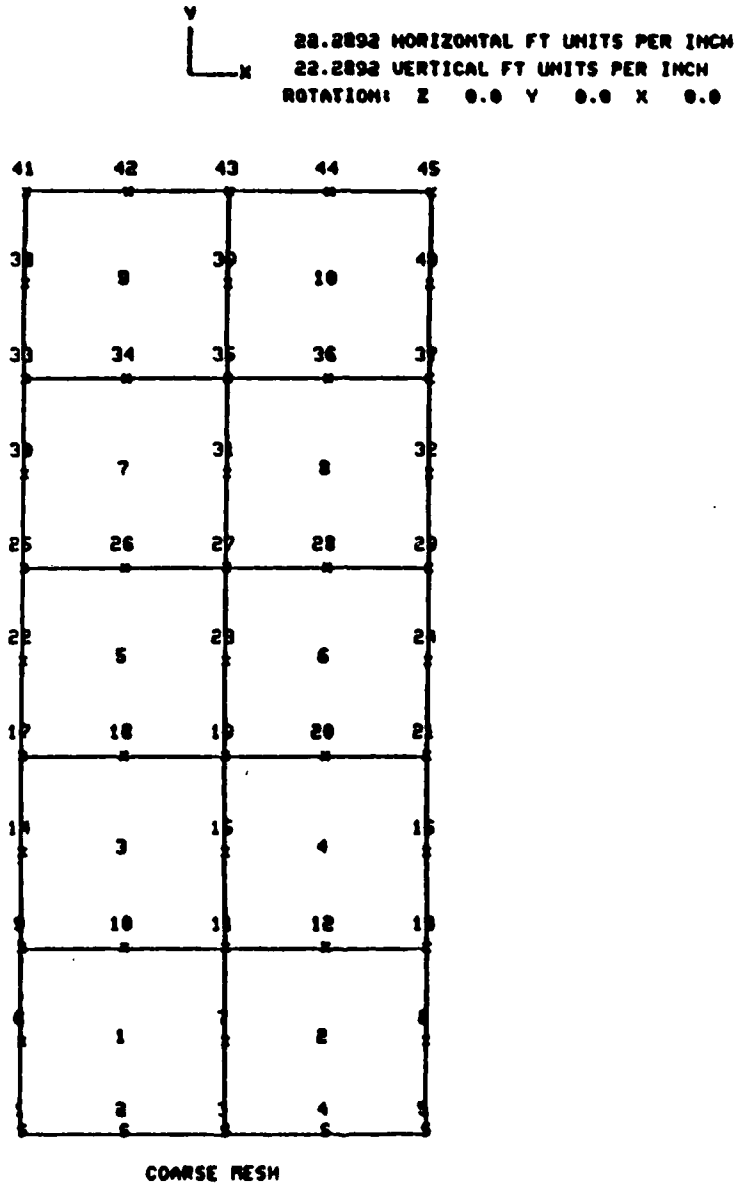

Figure 2. Mesh 1 used for Cases A1 and A2

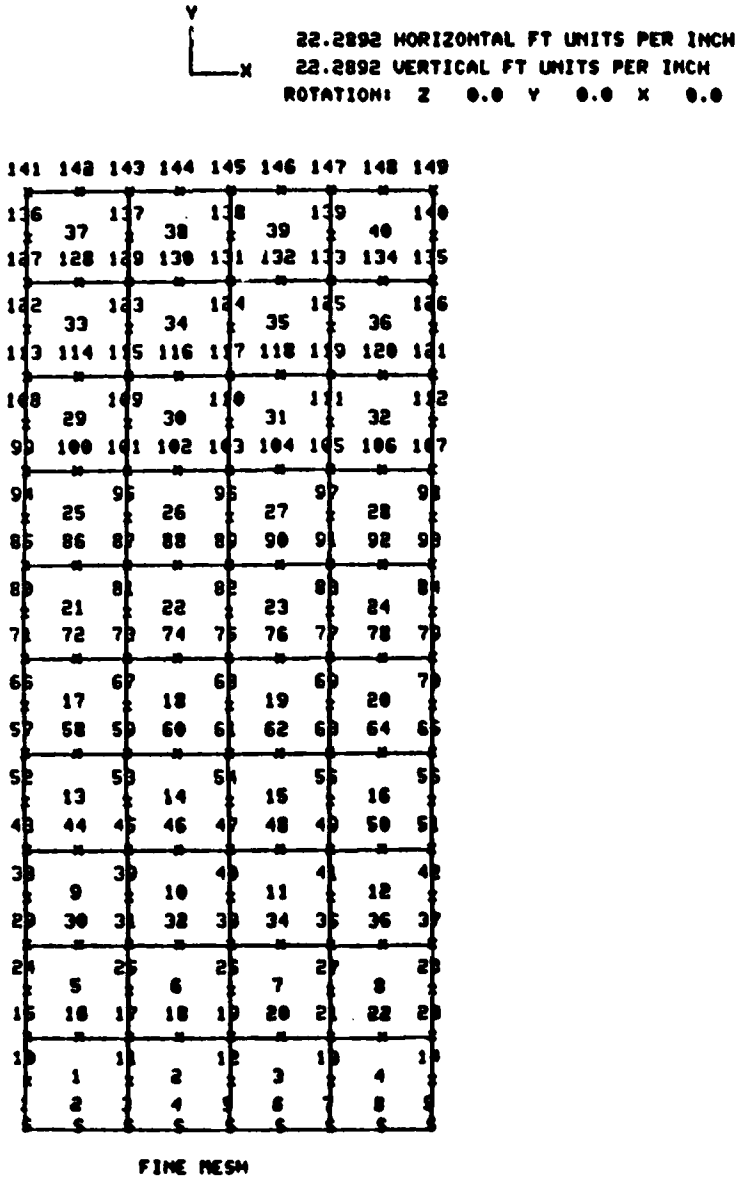

Figure 3. Mesh 2 used for Cases A1 and A2

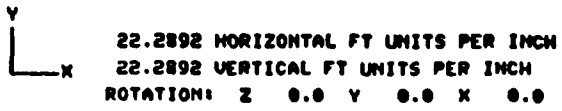

153	154	155	156	157	158	159	160
145	146	147	148	149	150	151	152
137	138	139	140	141	142	143	144
129	130	131	132	133	134	135	136
121	122	123	124	125	126	127	128
113	114	115	116	117	118	119	120
105	106	107	108	109	110	111	112
97	98	99	100	101	102	103	104
89	90	91	92	93	94	95	96
81	82	83	84	85	86	87	88
73	74	75	76	77	78	79	80
65	66	67	68	69	70	71	72
57	58	59	60	61	62	63	64
49	50	51	52	53	54	55	56
41	42	43	44	45	46	47	48
33	34	35	36	37	38	39	40
25	26	27	28	29	30	31	32
17	18	19	20	21	22	23	24
9	10	11	12	13	14	15	16
1	2	3	4	5	6	7	8

VERY FINE MESH WITH ELEMENTS LABELLED

Figure 4. Mesh 3 used for Cases A1 and A2
(Sheet 1 of 3)

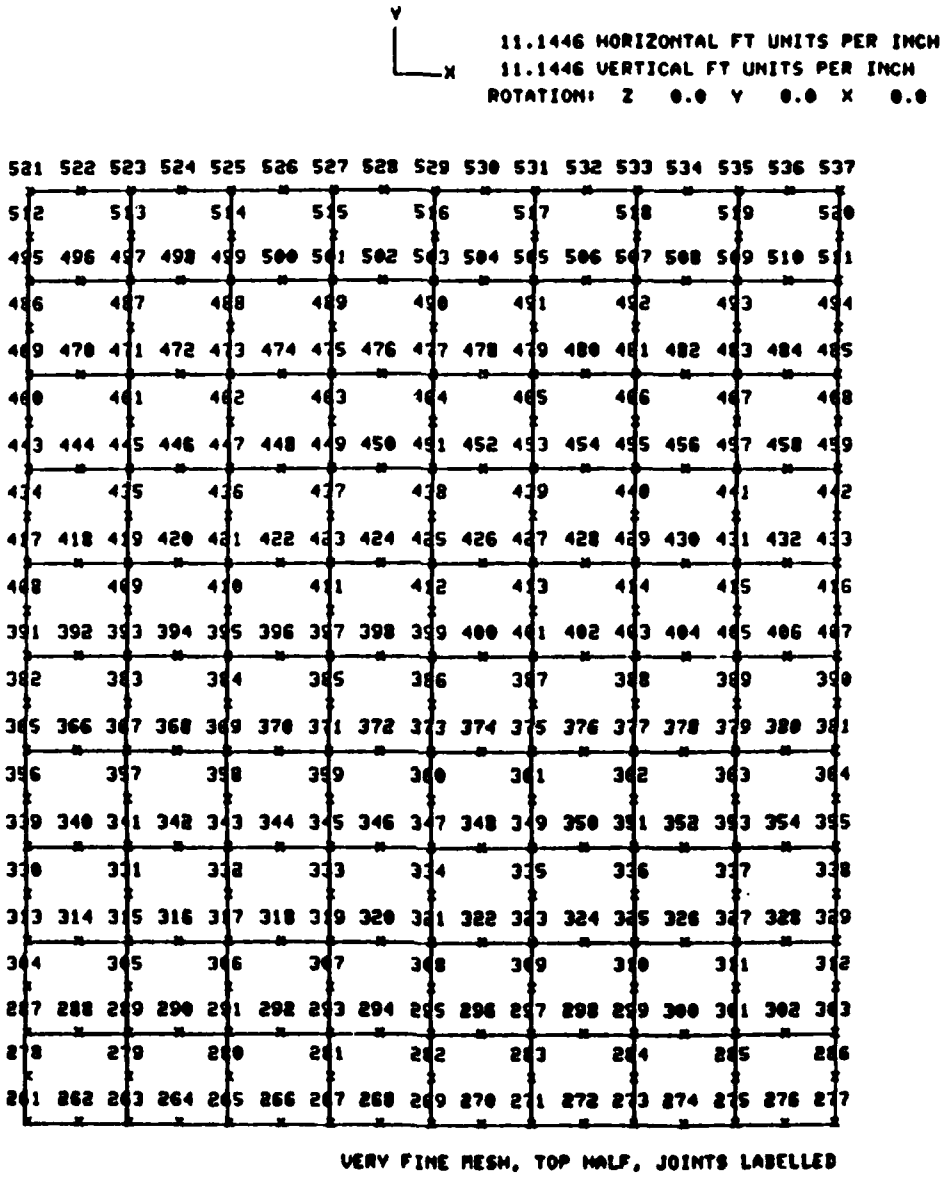

Figure 4. (Sheet 2 of 3)

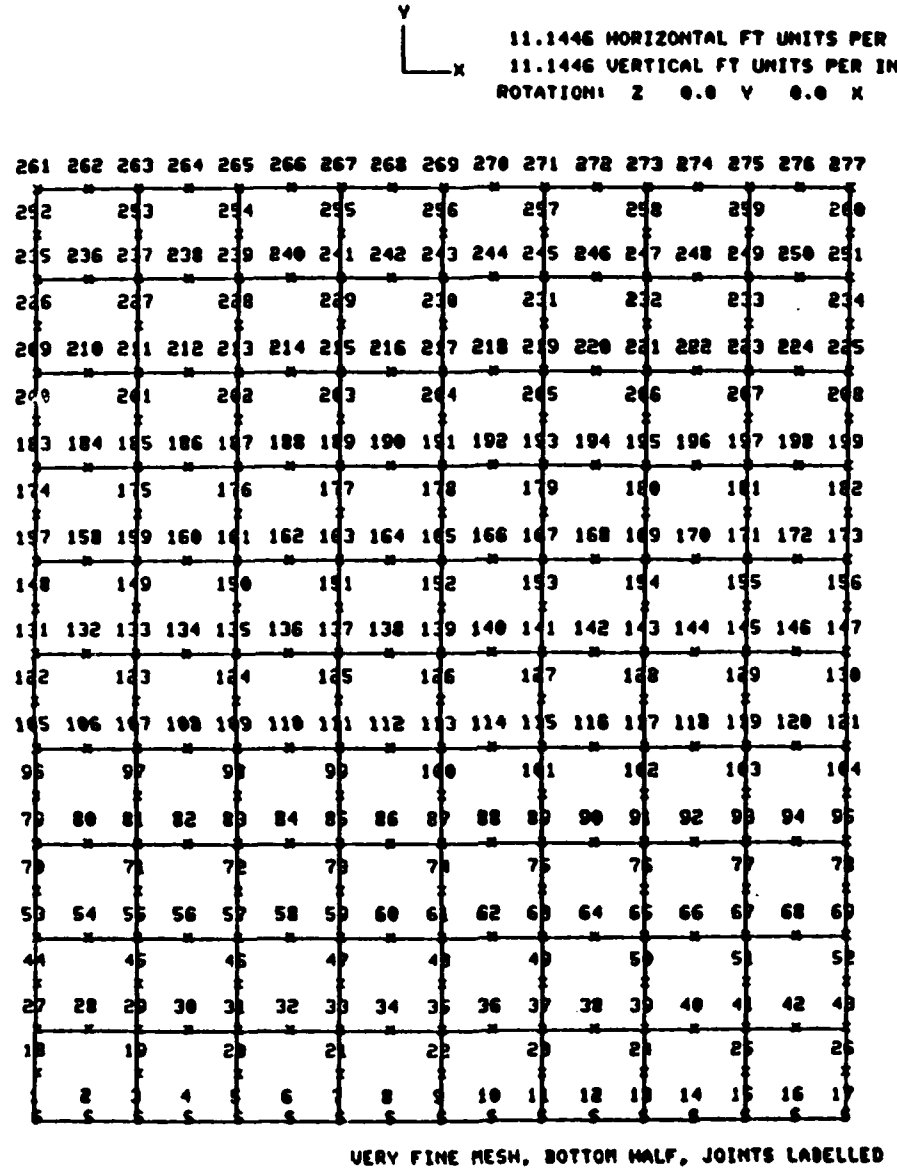

Figure 4. (Sheet 3 of 3)

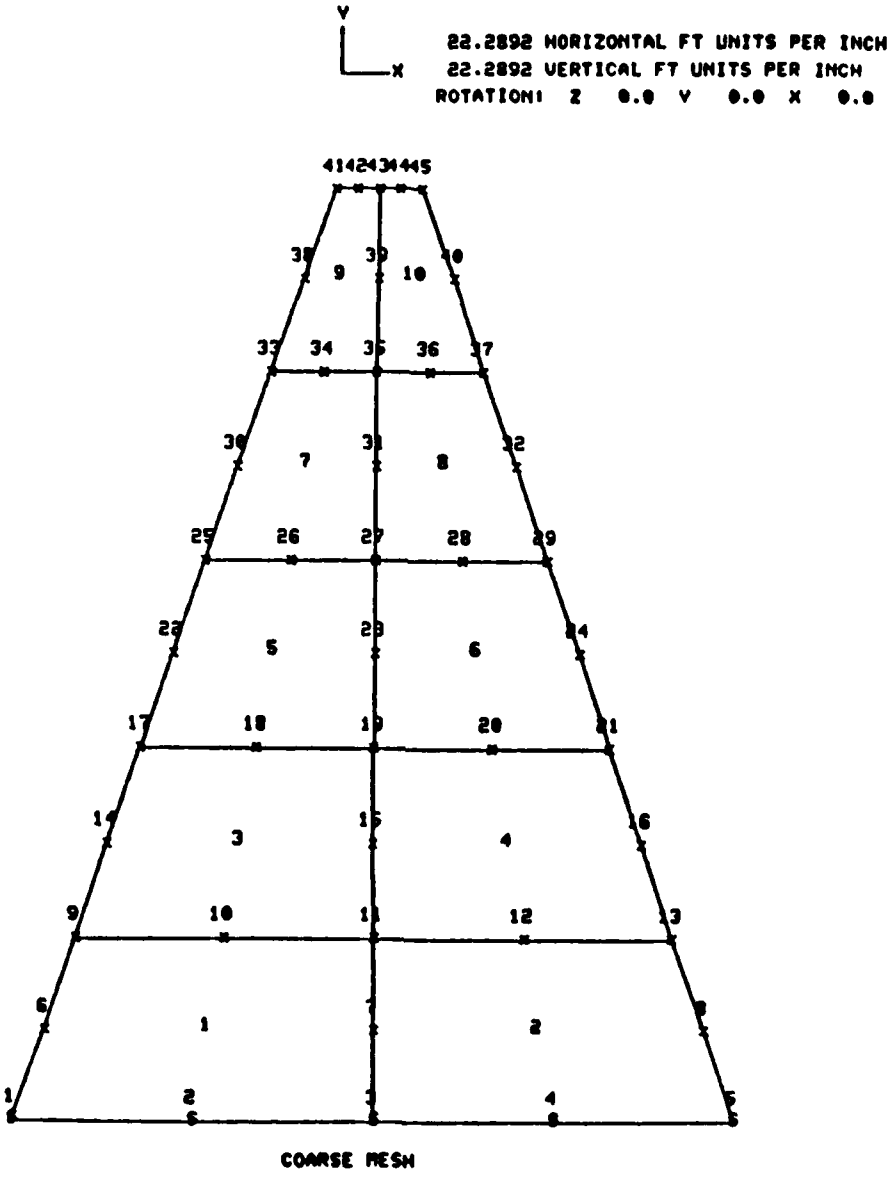

Figure 5. Mesh 1 used for Cases B1 and B2

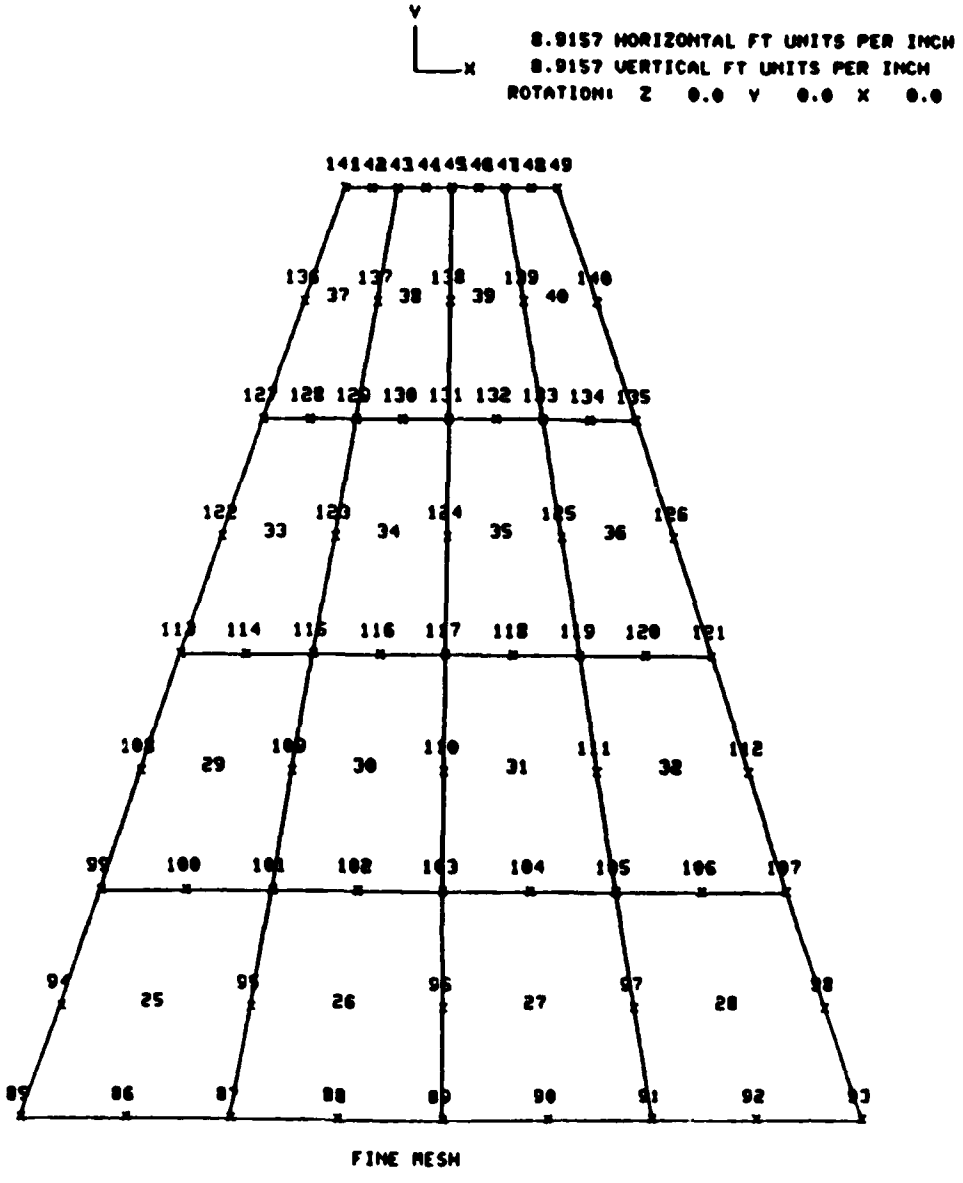

Figure 6. Mesh 2 used for Cases B1 and B2 (enlarged plot of top four rows of elements of Mesh 2) (Continued)

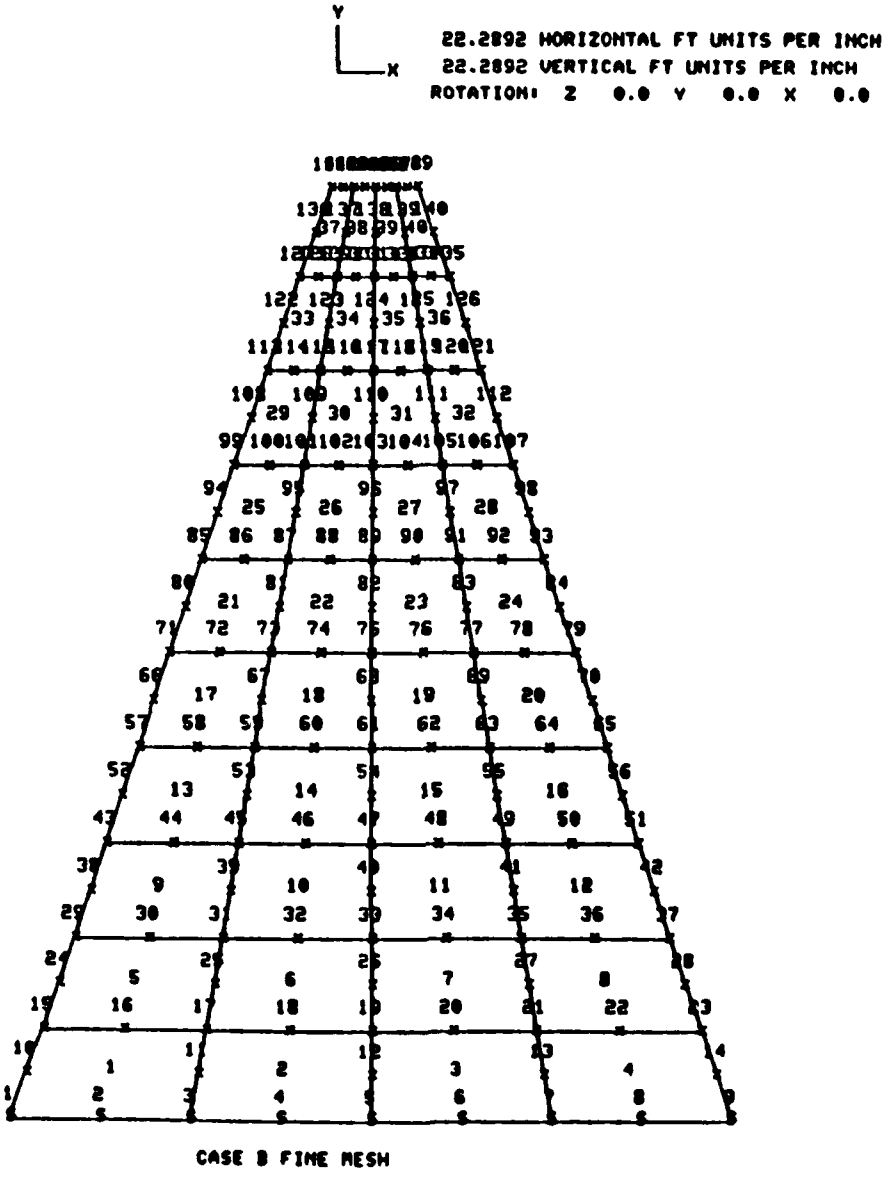

Figure 6. (Concluded)

as possible with Timoshenko Beam Theory boundary conditions for flexure and minimal normal stress in the x direction.

Output

17. Deflections and reactions were obtained for all meshes and loadings. The stresses were output in two different forms: (1) for each element for each node, and (2) averaged at each node. The first form of output is useful in understanding the accuracy of the model but generates a tremendous amount of output depending on the size of the model. Differences in the nodal values for a common node provide one criteria for determining the accuracy of the model. The second form of the output, the average stresses at a node, produced only one line of output per joint and provides a quicker means of assessing the stress magnitude and distribution. The second form of output is also used by the stress contouring capability of GTSTRUDL to produce contour plots of the stress components.

18. The input used for mesh 2 for Cases A1, A2, B1, and B2 is presented in Appendix A.

Comparison of Finite Element Results and Closed-Form Results

19. For the two structures considered, GTSTRUDL results for the deflections, SYY, and SXY stresses were compared to Timoshenko Beam Theory and Theory of Elasticity solutions. A closed-form solution could not be found for the trapezoidal cantilevers with a linear varying load, therefore only GTSTRUDL results are presented for this case. The equations used to generate the results for the closed-form solutions are presented in Appendix B. The Timoshenko Beam Theory solution includes the effect of shear deformation which is significant due to the relatively short and deep characteristics of the two beam-type structures.

Comparison of Results for Rectangular Cantilever

20. A comparison of the transverse deflection results along the height of the rectangular beam is presented in Table 1 for the load at the top of the beam (Case A1). The deflection results agree well for all meshes near the tip of the beam when compared with the Theory of Elasticity solution. However, the finite element results are more flexible near the base of the beam. The

Table 1

Comparison of Deflections of Rectangular Cantilever With Load at the Top (Case A1)

Distance from Base, ft	Deflection at Center Line, in.				
	Mesh 1	Mesh 2	Mesh 3	Timoshenko Beam Theory	Theory of Elasticity Solution
18.5	0.0360	0.0492	0.0564	0.0288	0.0324
37.0	0.0960	0.1056	0.1140	0.0852	0.0924
55.5	0.1800	0.1884	0.1956	0.1668	0.1776
74.0	0.2832	0.2916	0.2988	0.2688	0.2832
92.5	0.4056	0.4128	0.4212	0.3900	0.4092
74.0	0.0236	0.0243	0.0249	0.0224	0.0236
92.5	0.0338	0.0344	0.0351	0.0325	0.0341
111.0	0.0453	0.0459	0.0466	0.0439	0.0458
129.5	0.0577	0.0584	0.0591	0.0564	0.0585
148.0	0.0710	0.0717	0.0723	0.0696	0.0720
166.5	0.0848	0.0855	0.0861	0.0833	0.0860
185.0	1.1832	1.1916	1.2000	1.1676	1.2036

Timoshenko Beam Theory solution is not only stiffer than the finite element solution but also stiffer than the Theory of Elasticity solution. These results indicate that even mesh 1 produces reasonably accurate results for the deflection.

21. A comparison of the SXY (shear) and SYY (normal) stresses was made at two elevations of the beam for Case A1. The results for these stresses for the various meshes at a height of 37.0 ft above the base are presented in Table 2 while a comparison of these stresses at a height of 111.0 ft above the base is presented in Table 3. Timoshenko Beam Theory and the Theory of Elasticity solutions produced the same stresses for Case A1.

22. The SYY stresses at a height of 37.0 ft converged to a value somewhat higher than the closed-form solution at the boundaries ($x = \pm 40$ ft). However, the results were within 2 percent of the closed-form solution. The results for SYY changed less than 2 percent over the three meshes indicating that the normal stress converges very fast.

Table 2

Comparison of Stresses for a Rectangular Cantilever with Load at the Top (Case A1) at Height of 37 Ft

	SYY, psi			
x, ft	Mesh 1	Mesh 2	Mesh 3	Closed Form*
-40.0	970.25	979.72	977.18	963.54
-30.0		724.56	724.58	722.66
-20.0	468.20	475.33	472.49	481.77
-10.0		225.23	231.01	240.89
0.0	0.00	0.00	0.00	0.00
10.0		-225.23	-231.01	-240.89
20.0	-468.20	-475.33	-472.49	-481.77
30.0		-724.56	-724.58	-722.66
40.0	-970.25	-979.72	-977.18	-963.54
	SXY, psi			
	Mesh 1	Mesh 2	Mesh 3	Closed Form*
-40.0	61.73	6.97	2.97	0.00
-30.0		62.01	66.40	56.97
-20.0	93.49	109.58	102.81	97.66
-10.0		117.80	117.63	122.07
0.0	134.97	122.24	120.66	130.21
10.0		117.80	117.63	122.07
20.0	93.49	109.58	102.81	97.66
30.0		62.01	66.40	56.97
40.0	61.73	6.97	2.97	0.00

* Theory of Elasticity and Timoshenko Beam Theory stresses are the same for this case.

23. The shear stress, SXY, on the other hand, required a much finer mesh to predict the classical parabolic distribution. The IPQQ element can only represent a linear variation of strain along the edges, therefore mesh 1 did not produce accurate results. In fact, mesh 3 was only within 8 percent of predicting the maximum shear stress. The slow convergence of the shear stress may be due to boundary effects at the base, since the rollers are forcing all of the shear to the center node at the base in each mesh.

24. The stresses (SXY and SYY) at 111.0 ft above the base converge more

Table 3

Comparison of Stresses for a Rectangular Cantilever with Load at the Top (Case A1) at Height of 111 Ft

	SYY, psi			
x, ft	Mesh 1	Mesh 2	Mesh 3	Closed Form*
-40.0	481.11	481.65	481.77	481.77
-30.0		361.40	361.38	361.33
-20.0	241.20	240.92	240.84	240.89
-10.0		120.35	120.35	120.44
0.0	0.00	0.00	0.00	0.00
10.0		-120.35	-120.35	-120.44
20.0	-241.20	-240.92	-240.84	-240.89
30.0		-361.40	-361.38	-361.33
40.0	-481.11	-481.65	-481.77	-481.77
	SXY, psi			
	Mesh 1	Mesh 2	Mesh 3	Closed Form*
-40.0	27.37	6.81	1.72	0.00
-30.0		56.31	58.58	56.97
-20.0	95.31	104.47	99.31	97.66
-10.0		121.60	123.88	122.07
0.0	157.85	137.21	132.10	130.21
10.0		121.60	123.88	122.07
20.0	95.31	104.47	99.31	97.66
30.0		56.31	58.58	56.97
40.0	27.37	6.81	1.72	0.00

* Theory of Elasticity and Timoshenko Beam Theory stresses are the same for this case.

rapidly than those at 37.0 ft; especially the shear stress. Mesh 1 continues to produce highly erroneous results for SXY, indicating that mesh 2 is required for an accurate shear stress distribution.

25. Another useful interpretative tool available in most finite element programs is the stress contour plot. GTSTRUDL SXY contour plots are presented in Figures 7 through 9 for the three meshes. As can be seen from these plots, the boundary restraint at the center of the base significantly affects the SXY contour near the base. Contour plots for the SYY stress were not obtained

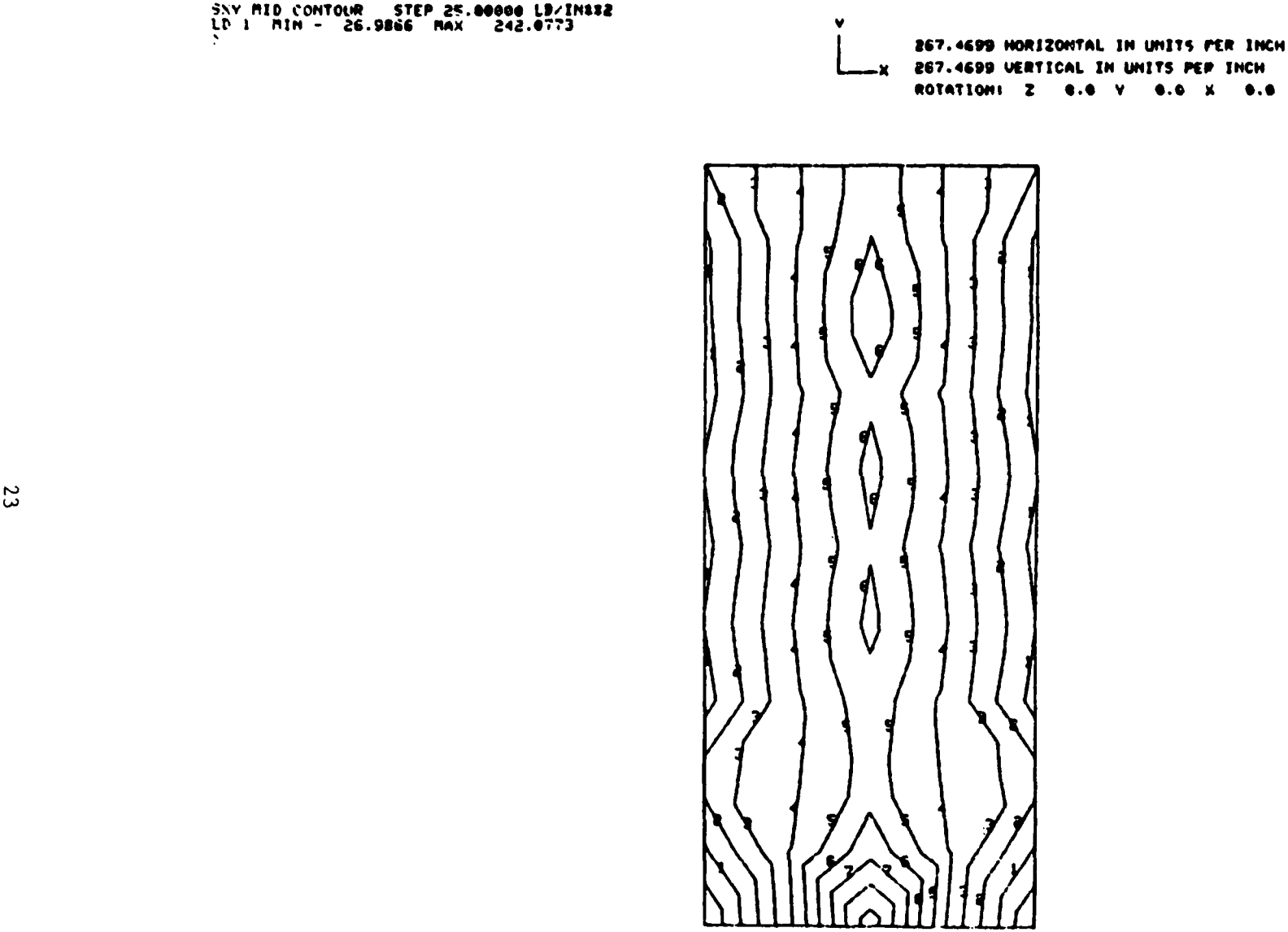

Figure 7. SXY contour plot, Case A1, mesh 1

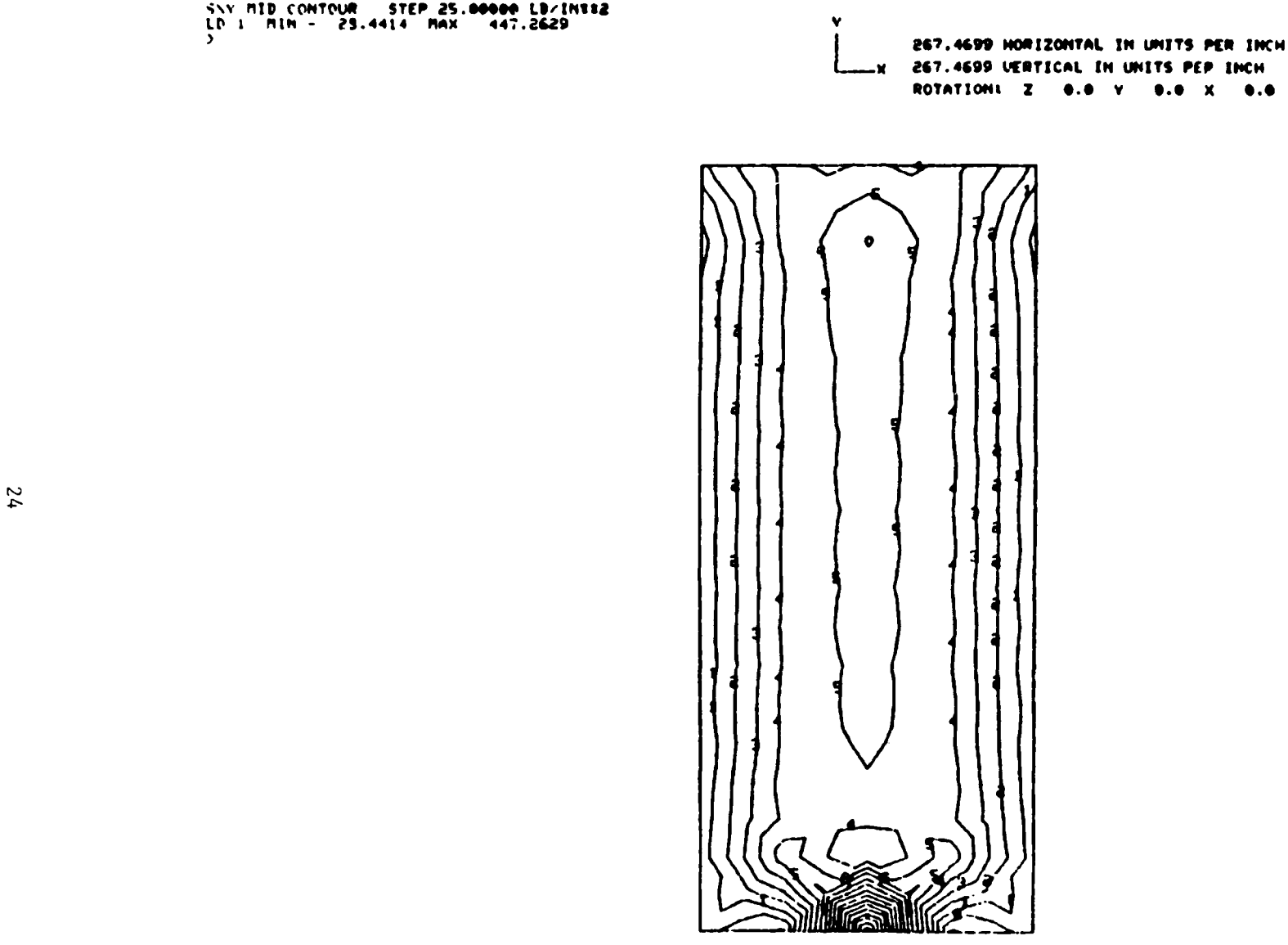

Figure 8. SXY contour plot, Case A1, mesh 2

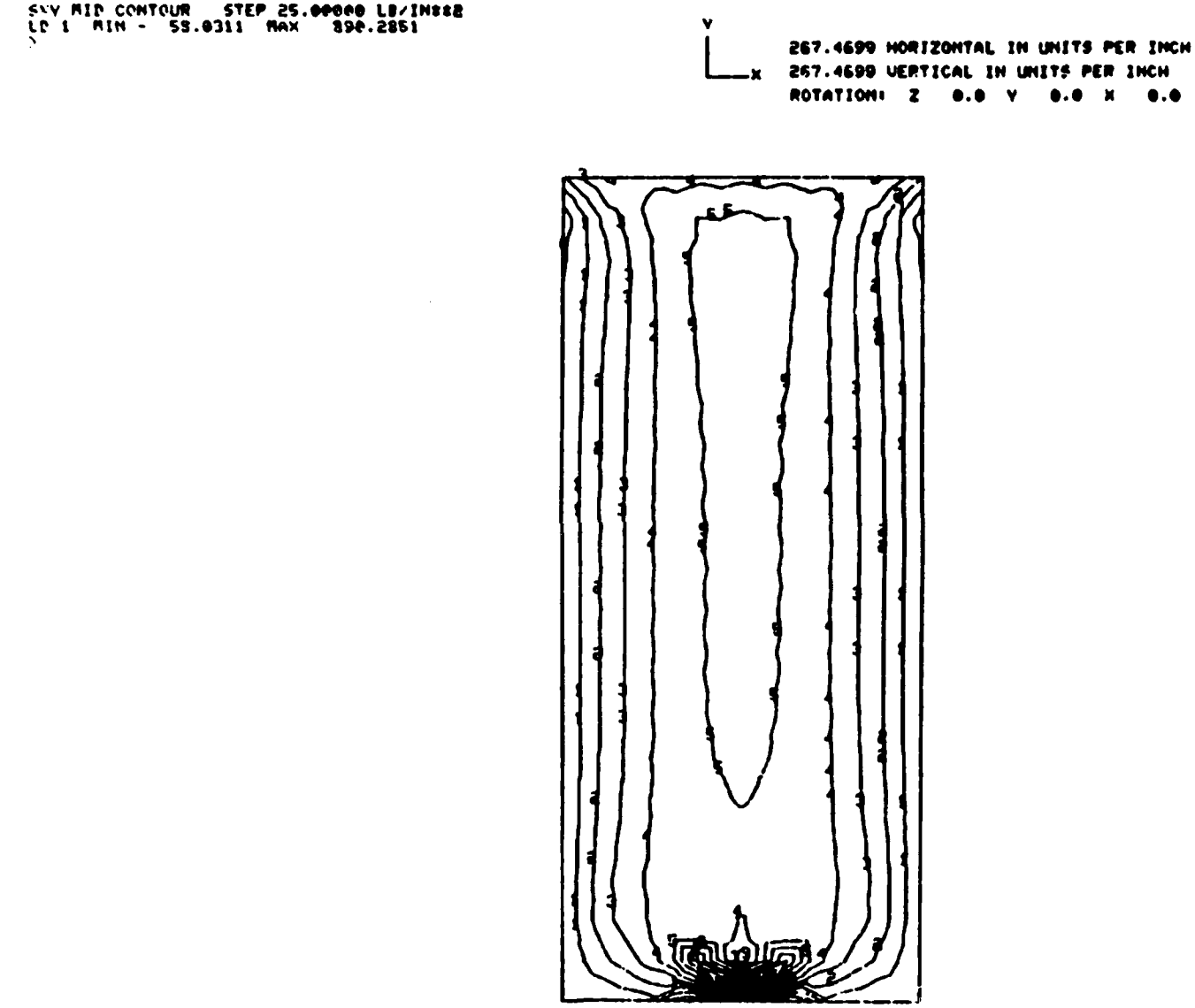

Figure 9. SXY contour plot, Case A1, mesh 3

since convergence to the correct solution was obtained very quickly.

26. Next, results were analyzed for Case A2, the rectangular cantilever beam with a linearly varying load over the height. Table 4 summarizes the transverse deflection results over the height at the center line. The deflection results are very similar to those in Case A1 with the Timoshenko Beam Theory results stiffer than the finite element results and the finite element results higher near the base and lower at the top than the Theory of Elasticity results.

Table 4

Comparison of Deflections of Rectangular Cantilever with Linear Load (Case A2)

Distance from Base, ft	Deflection at Center Line, in.				
	Mesh 1	Mesh 2	Mesh 3	Timoshenko Beam Theory	Theory of Elasticity
18.5	0.0312	0.0396	0.0480	0.0180	0.0240
37.0	0.0564	0.0636	0.0720	0.0420	0.0540
55.5	0.0828	0.0912	0.0996	0.0684	0.0852
74.0	0.1116	0.1200	0.1272	0.0972	0.1188
92.0	0.1416	0.1488	0.1572	0.1272	0.1524
111.0	0.1704	0.1788	0.1872	0.1560	0.1860
129.5	0.1992	0.2076	0.2160	0.1848	0.2184
148.0	0.2280	0.2352	0.2436	0.2148	0.2508
166.5	0.2556	0.2640	0.2712	0.2412	0.2820
185.0	0.2832	0.2904	0.2988	0.2688	0.3132

27. Again, SXY and SYY stresses were compared for the various solutions at two heights of the beam for Case A2. The results for the various meshes and the closed-form solutions at a height 37.0 ft above the base are presented in Table 5 and the results at 111.0 ft above the base are presented in Table 6.

28. Stress results for Case A2 were very similar to those of Case A1 with respect to convergence characteristics. Again, the normal stress, SYY, converged very rapidly at both elevations while the shear stress, SXY, required a finer mesh. Boundary conditions near the base appeared to affect the SXY stress more than the SYY stress. Mesh 2 provided an accurate representation of the normal stress at both elevations, while mesh 3 was required to

Table 5

Comparison of Stresses for a Rectangular Cantilever with Linear Load (Case A2) at a Height of 37 Ft

	SYY, psi				
x, ft	Mesh 1	Mesh 2	Mesh 3	Timoshenko Beam Theory	Theory of Elasticity
-40.0	203.98	218.65	217.43	219.49	206.67
-30.0		165.74	166.28	164.63	165.52
-20.0	99.94	108.90	106.65	109.75	115.36
-10.0		46.04	52.40	54.88	59.18
0.0	0.00	0.00	0.00	0.00	0.00
10.0		-46.04	-52.40	-54.88	-59.18
20.0	-99.94	-108.90	-106.65	-109.75	-115.36
30.0		-165.74	-166.28	-164.63	-165.52
40.0	-203.98	-218.65	-217.43	-219.49	-206.67
	SXY, psi				
	Mesh 1	Mesh 2	Mesh 3	Timoshenko Beam Theory	Theory of Elasticity
-40.0	54.25	4.42	2.40	0.00	0.00
-30.0		44.09	47.79	38.93	38.59
-20.0	62.79	76.30	71.32	66.74	66.65
-10.0		79.26	78.24	83.42	83.70
0.0	83.02	78.31	78.81	88.99	89.42
10.0		79.26	78.24	83.42	83.70
20.0	62.79	76.30	71.32	66.74	66.65
30.0		44.09	47.79	38.93	38.59
40.0	54.25	4.42	2.40	0.00	0.00

produce an accurate shear stress near the base with mesh 2 yielding an accurate shear stress away from the base.

Comparison of Results for Trapezoidal Cantilever

29. Meshes 1 and 2 only were used in the analysis of the trapezoidal cantilever. While mesh 3 for the rectangular cantilever produced more accurate shear stresses near the base, the additional cost was not felt to be

Table 6

Comparison of Stresses for a Rectangular Cantilever with Linear Load (Case A2) at a Height of 111 Ft

	SYY, psi				
x, ft	Mesh 1	Mesh 2	Mesh 3	Timoshenko Beam Theory	Theory of Elasticity
-40.0	15.31	18.36	19.11	27.44	21.02
-30.0		20.10	20.40	20.58	21.03
-20.0	16.49	16.76	17.17	13.72	16.53
-10.0		10.83	10.94	6.86	9.01
0.0	0.00	0.00	0.00	0.00	0.00
10.0		-10.83	-10.94	-6.86	-9.01
20.0	-16.49	-16.76	-17.17	-13.72	-16.53
30.0		-20.10	-20.40	-20.58	-21.03
40.0	-15.31	-18.36	-19.11	-27.44	-21.02
	SXY, psi				
	Mesh 1	Mesh 2	Mesh 3	Timoshenko Beam Theory	Theory of Elasticity
-40.0	4.01	0.74	0.17	0.00	0.00
-30.0		9.12	9.42	9.74	9.39
-20.0	15.71	17.29	16.69	16.69	16.60
-10.0		21.00	21.43	20.85	21.13
0.0	26.69	24.02	23.33	22.24	22.68
10.0		21.00	21.43	20.85	21.13
20.0	15.71	17.29	16.69	16.69	16.60
30.0		9.12	9.42	9.74	9.38
40.0	4.01	0.74	0.17	0.00	0.00

justified. As mentioned previously, closed-form results were found only for the concentrated load at the top (Case B1). Case B2 was executed in order to compare the results of meshes 1 and 2.

30. Meshes 1 and 2 for the trapezoidal cantilever were shown previously in Figures 5 and 6, respectively. Again, the meshes were equally subdivided horizontally and vertically for ease of generation. Only the coordinates at the four corners of the trapezoid had to be changed to modify the input of the rectangular cantilevers.

31. A comparison of the transverse deflection results along the height of the trapezoidal beam at its center line is presented in Table 7. Closed-form results for Timoshenko Beam Theory and Theory of Elasticity solutions are also presented in Table 7. For the trapezoidal cantilever, the results from the Timoshenko Beam Theory solution are stiffer than those from the Theory of Elasticity solution. This stiffer characteristic is greater in the trapezoidal cantilever than in the rectangular cantilever. Both mesh 1 and mesh 2 produce displacements at the top of the cantilever within 5 percent of the elasticity solution. Again, both meshes produce higher results near the base but lower results near the top when compared with the elasticity solution.

Table 7

Comparison of Deflections of Trapezoidal Cantilever with Concentrated Load at Top (Case B1)

Distance from Base, ft	Deflection at Center Line, in.			
	Mesh 1	Mesh 2	Timoshenko Beam Theory	Theory of Elasticity
18.5	0.0216	0.0324	0.0108	0.0132
37.0	0.0432	0.0504	0.0288	0.0336
55.5	0.0684	0.0756	0.0552	0.0624
74.0	0.1032	0.1116	0.0936	0.1032
92.5	0.1524	0.1608	0.1440	0.1584
111.0	0.2208	0.2292	0.2136	0.2304
129.5	0.3120	0.3216	0.3060	0.3288
148.0	0.4392	0.4488	0.4332	0.4608
166.5	0.6216	0.6288	0.6108	0.6468
185.0	0.8700	0.8868	0.8628	0.9120

32. A comparison of the SXY (shear) and SYY (normal) stresses was made as in the Case A studies. The results for these stresses for the various meshes at a height of 37.0 ft above the base are presented in Table 8 while a comparison of the stresses at a height of 111.0 ft above the base is presented in Table 9. Timoshenko Beam Theory and the Theory of Elasticity solutions are also presented in Tables 8 and 9.

33. The most interesting observation that can be made concerning the stresses reported in Tables 8 and 9 is the discrepancy between the Beam Theory

Table 8

Comparison of Stresses for a Trapezoidal Cantilever with Concentrated Load at the Top (Case B1) at Height of 37 Ft

	SYY, psi			
x, ft	Mesh 1	Mesh 2	Timoshenko Beam Theory	Theory of Elasticity
-59.0	373.88	430.03	442.88	411.47
-44.25		332.64	332.16	333.89
-29.5	251.89	234.41	221.44	235.89
-14.75		109.99	110.72	122.21
0.00	0.00	0.00	0.00	0.00
14.75		-109.99	-110.72	-122.21
29.5	-251.89	-234.41	-221.44	-235.89
44.25		-332.64	-332.16	-333.89
59.0	-373.88	-430.03	-442.88	-411.47
	SXY, psi			
	Mesh 1	Mesh 2	Timoshenko Beam Theory	Theory of Elasticity
-59.0	143.37	135.67	0.00	140.40
-44.25		87.72	38.62	90.57
-29.5	50.83	43.33	66.21	49.65
-14.75		29.32	82.76	22.71
0.00	-12.32	1.66	88.28	13.29
14.75		29.32	82.76	22.71
29.5	50.83	43.33	66.21	49.65
44.25		87.72	38.62	90.57
59.0	143.37	135.67	0.00	140.40

stresses calculated from My/I and VQ/It and the stresses from the Theory of Elasticity solution. At both elevations, the finite element results are converging towards the Theory of Elasticity solution. Practicing engineers that are not familiar with the analysis of tapered beams will find that shear stresses on a horizontal plane are at a maximum near the extreme fibers. The finite element results again agree more closely at 111.0 ft than at 37.0 ft due to the effect of the boundary conditions at the base on the stresses at

Table 9

Comparison of Stresses for a Trapezoidal Cantilever with Concentrated Load at the Top (Case B1) at Height of 111 Ft

	SYY, psi			
x, ft	Mesh 1	Mesh 2	Timoshenko Beam Theory	Theory of Elasticity
-33.75	664.38	642.78	676.73	637.54
-25.31		510.55	507.54	509.89
-16.88	357.51	359.23	338.36	356.18
-8.44		183.13	169.18	183.13
0.00	0.00	0.00	0.00	0.00
8.44		-183.13	-169.18	-183.13
16.88	-357.51	-359.23	-338.36	356.18
25.31		-510.55	-507.54	-509.89
33.75	-664.38	-642.78	-676.73	-637.54
	SXY, psi			
	Mesh 1	Mesh 2	Timoshenko Beam Theory	Theory of Elasticity
-33.75	177.08	208.76	0.00	217.54
-25.31		143.90	67.51	146.13
-16.88	82.94	78.44	115.74	89.55
-8.44		52.00	144.67	53.16
0.00	-6.35	27.78	154.32	40.63
8.44		52.00	144.67	53.16
16.88	-82.94	78.44	115.74	89.55
25.31		143.90	67.51	146.13
33.75	177.08	208.76	0.00	217.54

37.0 ft. Contour plots for the SYY and SXY stresses for meshes 1 and 2 are presented in Figures 10 through 13.

34. Case B2 was also analyzed using GTSTRUDL. Closed-form Theory of Elasticity solutions for Case B2 were not found in the literature. Based on the error in the Timoshenko Beam Theory solutions from Case B1 and the realization that Case B2 would have similar error, it was decided to compare the results only from the finite element models using meshes 1 and 2.

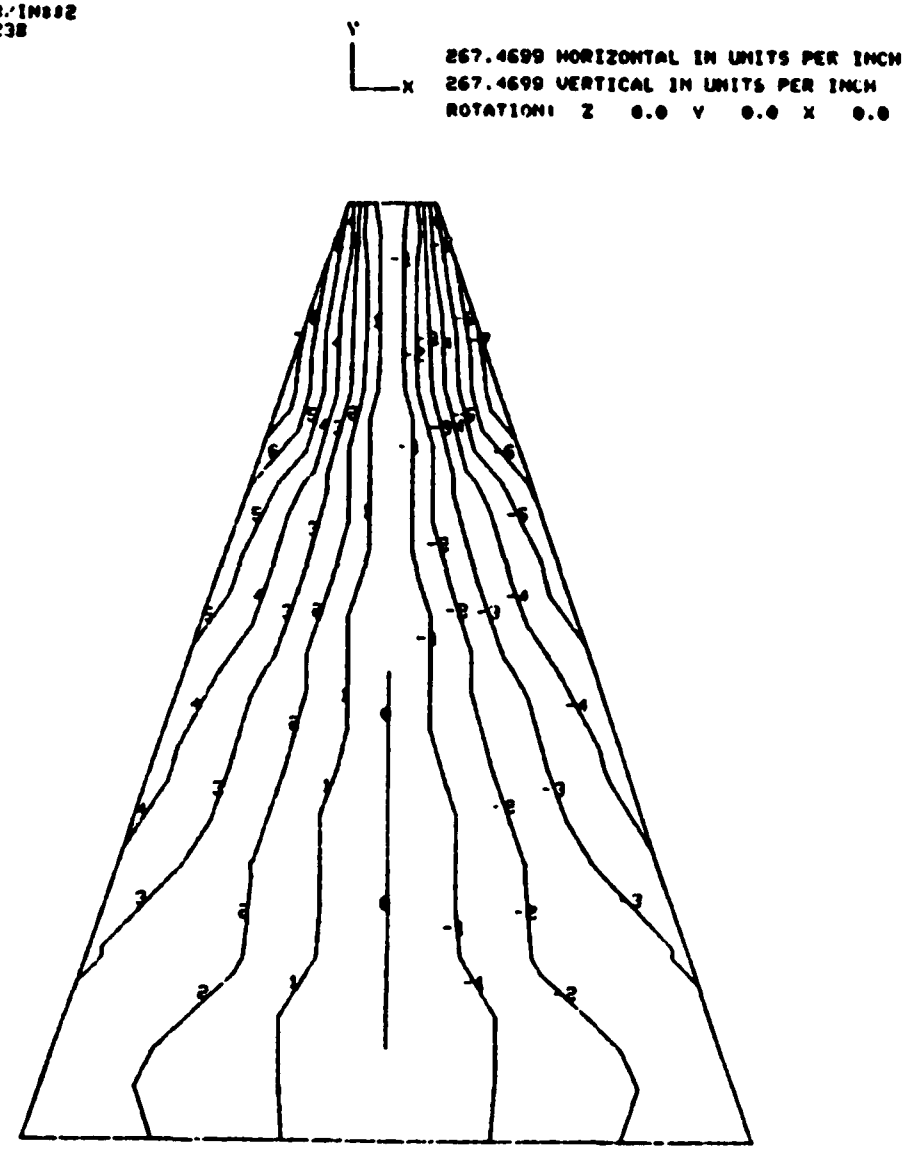

Figure 10. SXY contour plot, Case B1, mesh 1

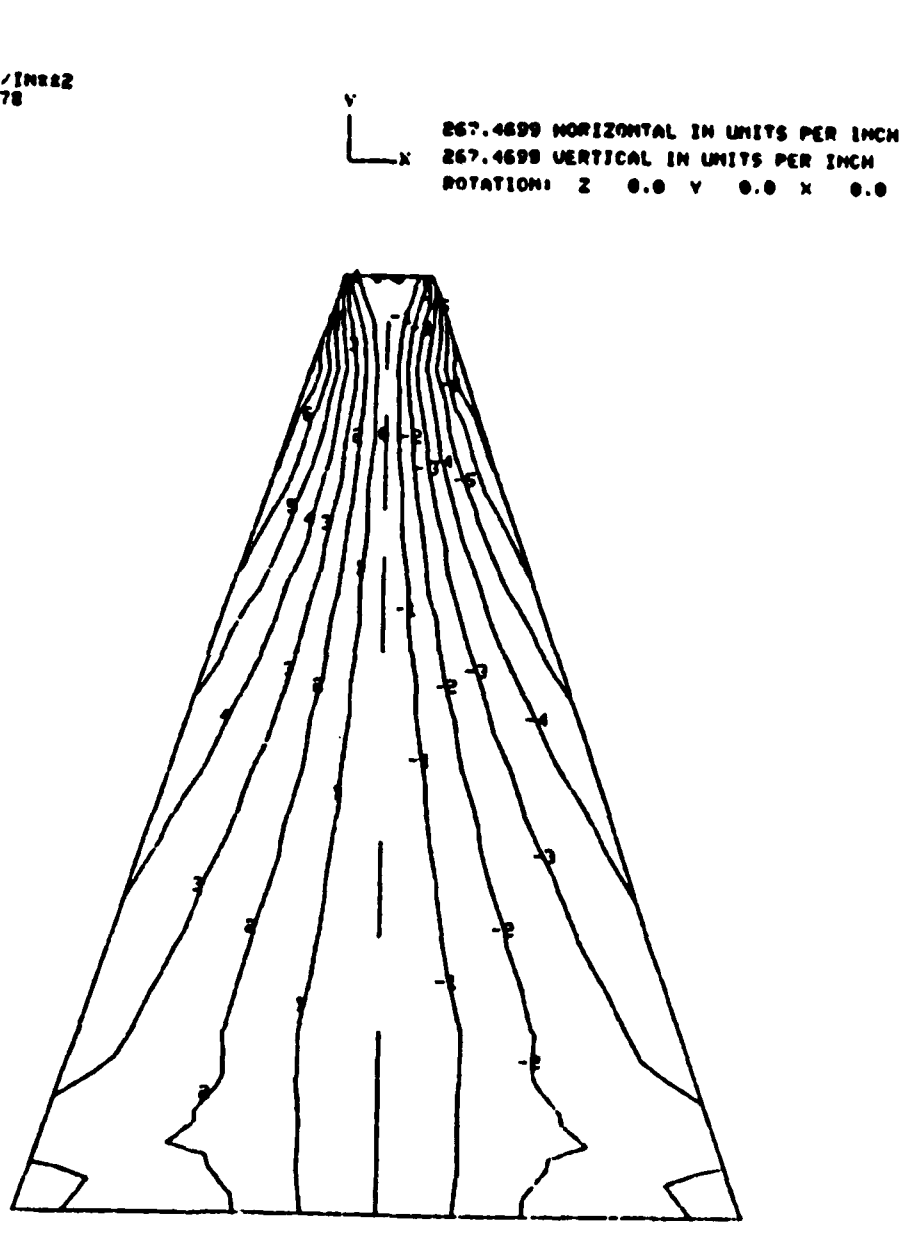

Figure 11. SYY contour plot, Case B1, mesh 2

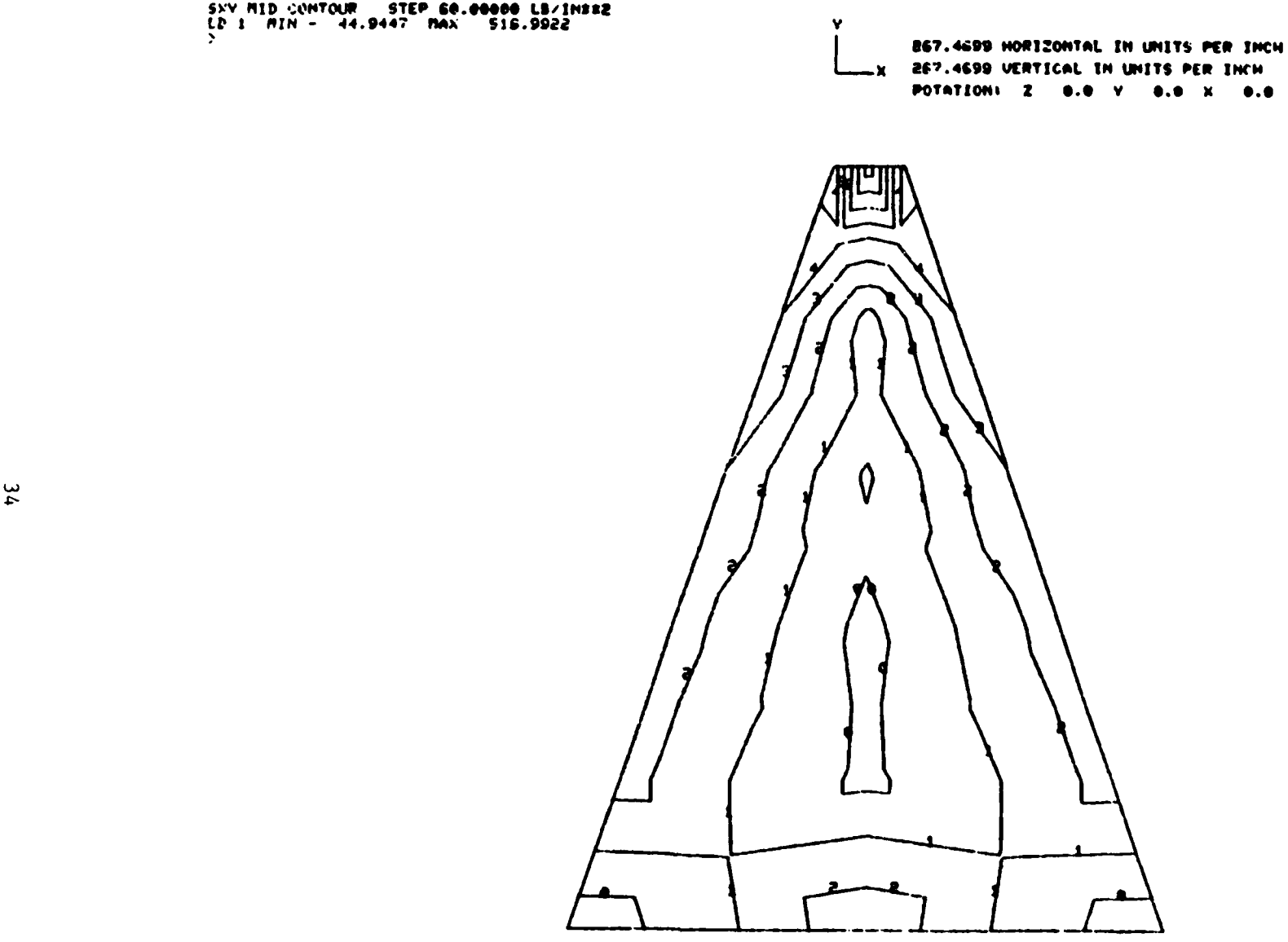

Figure 12. SXY contour plot, Case B1, mesh 1

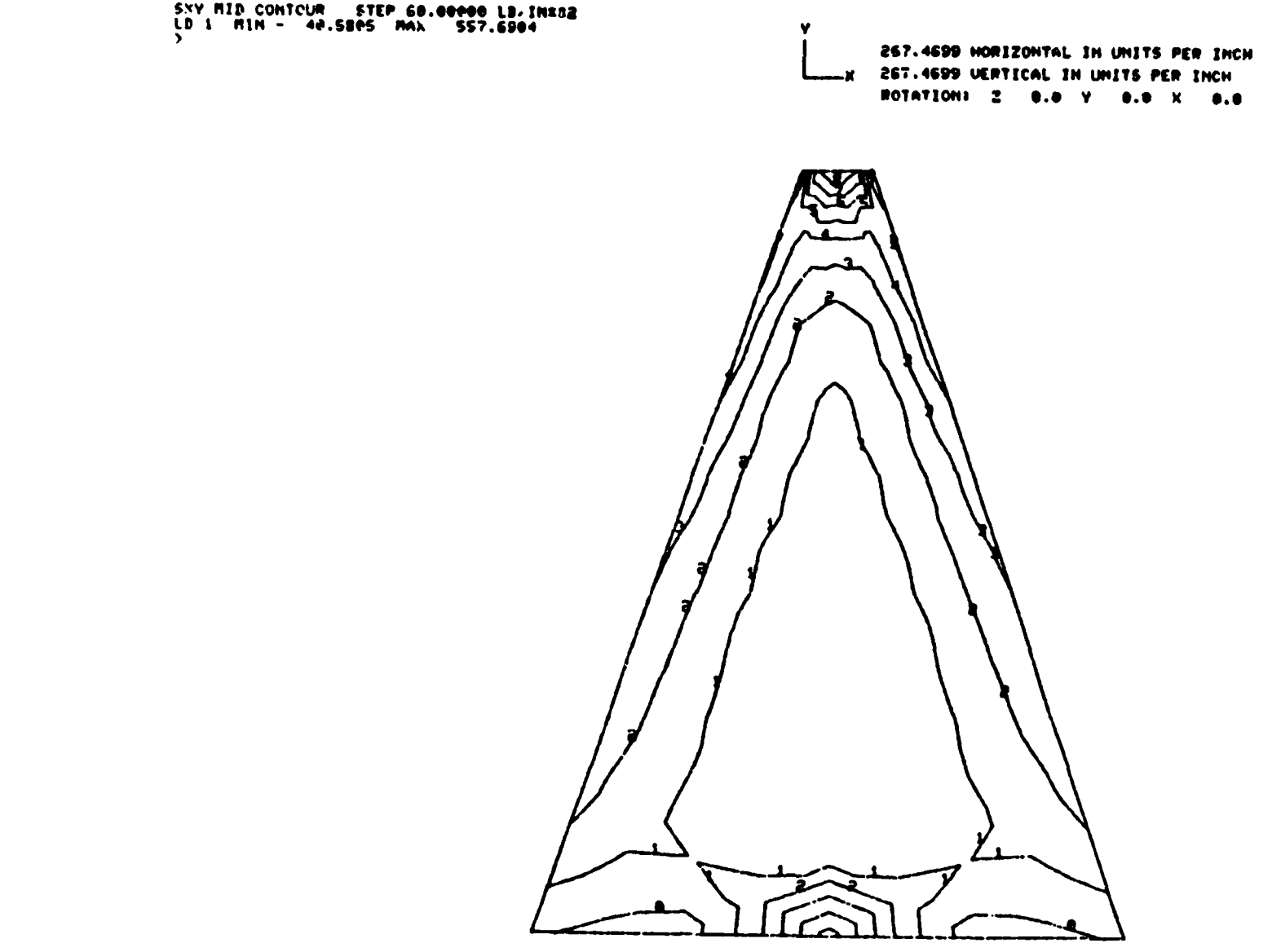

Figure 13. SXY contour plot, Case B1, mesh 2

35. A comparison of the deflection for meshes 1 and 2 is presented in Table 10. The difference in the maximum transverse displacement is approximately 7 percent with mesh 2 being more flexible as anticipated.

Table 10

Comparison of Deflection of Trapezoidal Cantilever with Linear Load (Case B2)

Distance from Base, ft	Deflection at Center Line, in.	
	Mesh 1	Mesh 2
18.5	0.0204	0.0324
37.0	0.0348	0.0420
55.5	0.0444	0.0516
74.0	0.0540	0.0624
92.5	0.0648	0.0732
111.0	0.0768	0.0852
129.5	0.0888	0.0972
148.0	0.1008	0.1092
166.5	0.1128	0.1212
185.0	0.1248	0.1332

36. Stresses were also computed for both meshes for Case B2. Again, a Theory of Elasticity solution was not found for the stresses Therefore, closed-form solutions were omitted in the comparison, since the Timoshenko Beam Theory solution was found to be erroneous in Case B1. The stresses at a height of 111.0 ft are shown in Table 11. Stresses at 37.0 ft were omitted since the boundary conditions significantly affect the results. At 111.0 ft, the SYY normal stresses changed less than 5 percent between the meshes, while the SXY shear stresses changed less than 10 percent. Again, note that the shear stress, SXY, is not zero on the tapered edges which is contrary to beam theory.

Conclusions Based on Simple Model Results

37. The results from Cases A1, A2, B1, and B2 indicate that mesh 2 with four elements across the base is a reasonable compromise between accuracy and

Table 11

Comparison of Stresses for a Trapezoidal Cantilever with Linear Load (Case B2) at Height of 111 Ft

x, ft	SYY, psi Mesh 1	Mesh 2
-33.75	35.93	37.20
-25.31		28.39
-16.88	19.89	19.63
-8.44		11.36
0.00	0.00	0.00
8.44		-11.36
16.88	-19.89	-19.63
25.31		-28.39
33.75	-35.93	-37.20
	SXY, psi	
	Mesh 1	Mesh 2
-33.75	14.32	13.13
-25.31		15.85
-16.88	17.82	18.44
-8.44		19.58
0.00	22.31	20.68
8.44		19.58
16.88	17.82	18.44
25.31		15.85
33.75	14.32	13.13

cost for the first model of a gravity dam using the IPQQ element. An important point to remember is that mesh 2 is only a starting point. Geometrical considerations such as the gallery areas in a dam can quickly cause changes to this guideline.

38. Two important conclusions can be drawn regarding the behavior of the simple models:

a. Boundary conditions at the base can cause stress concentrations that affect the solution over some height above the base. The SXY stress contour plots indicate the effect of forcing all the

shearing force into one point along the base. This is probably a more severe case than found in practice since the horizontal restraint from the foundation is over a large area of the base.

b. Timoshenko Beam Theory formulas provide reasonable approximations (within 10 percent for the cases in this study) for the normal stress distribution but are very inaccurate for the shear stress distribution. Care must be exercised when using these formulas in practice.

PART III: FINITE ELEMENT ANALYSIS OF DAM MONOLITH

Description of Structure

39. As discussed previously, a typical nonoverflow monolith similar to the RBR Dam was the structure chosen for the finite element analysis. The geometry of the monolith is shown in Figure 14. The monolith was assumed to be completely restrained along the base. The structure was loaded by a hydrostatic loading beginning at 170 ft above the base and the self-weight of the concrete of 150 pcf.

Modeling Procedure

40. The results presented in Part II for the rectangular and trapezoidal cantilevers indicated that a mesh with four elements across the base was a reasonable compromise between accuracy and cost. Therefore, the first model for the monolith, mesh RBR4, had four eight-noded IPQQ elements across the base. The mesh was graded to facilitate automatic generation since an engineer's time is often more costly than computational resources in a finite element analysis. The tapered sides of the monolith were also approximated to facilitate the automatic generation. Mesh RBR4 is shown in Figure 15. The mesh contained 28 elements and 107 nodes. Before performing the two-dimensional (2D) analysis, the basic assumption of whether to do a plane stress or plane strain analysis must be made. Plane stress is usually applicable for 2D models with a thickness which is small compared to the other two structural dimensions. On the other hand, a plane strain analysis is usually applicable for structures with a thickness which is large compared to the other structural dimensions. Although most dams are thick (long) when compared to the dimensions of a cross section, the vertical construction joints between monoliths do not provide complete transfer of forces across the joint boundaries. Therefore, the model was assumed to be in a state of plane stress. A comparison of plane stress versus plane strain is presented in paragraphs 46 and 47. The monolith was analyzed for the combined effects of the hydrostatic and self-weight (body-force) loading. The results were interpreted by obtaining contour plots of the SXX, SYY, and SXY stress components. The contour plots are shown in Figures 16 through 18.

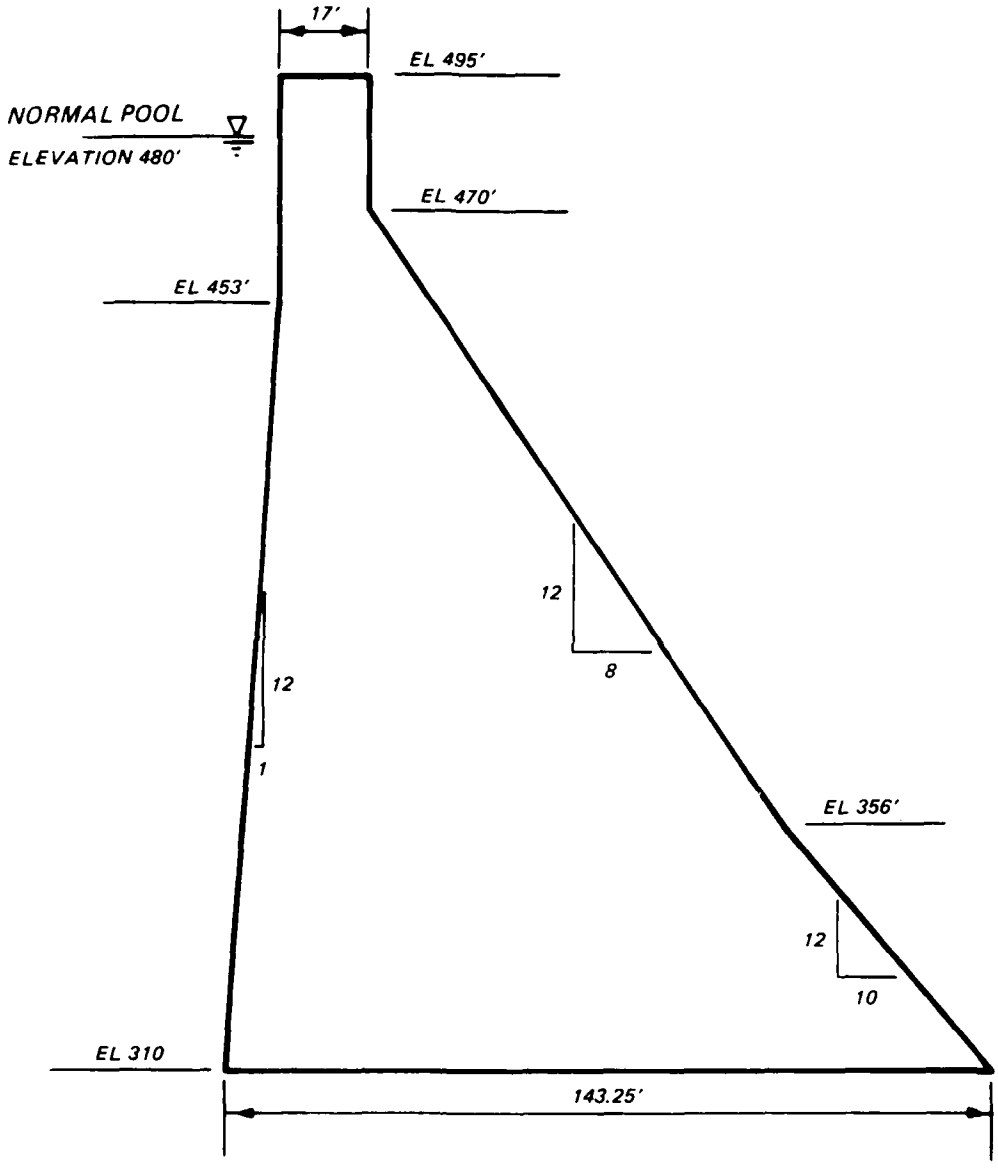

Figure 14. Geometry of dam monolith

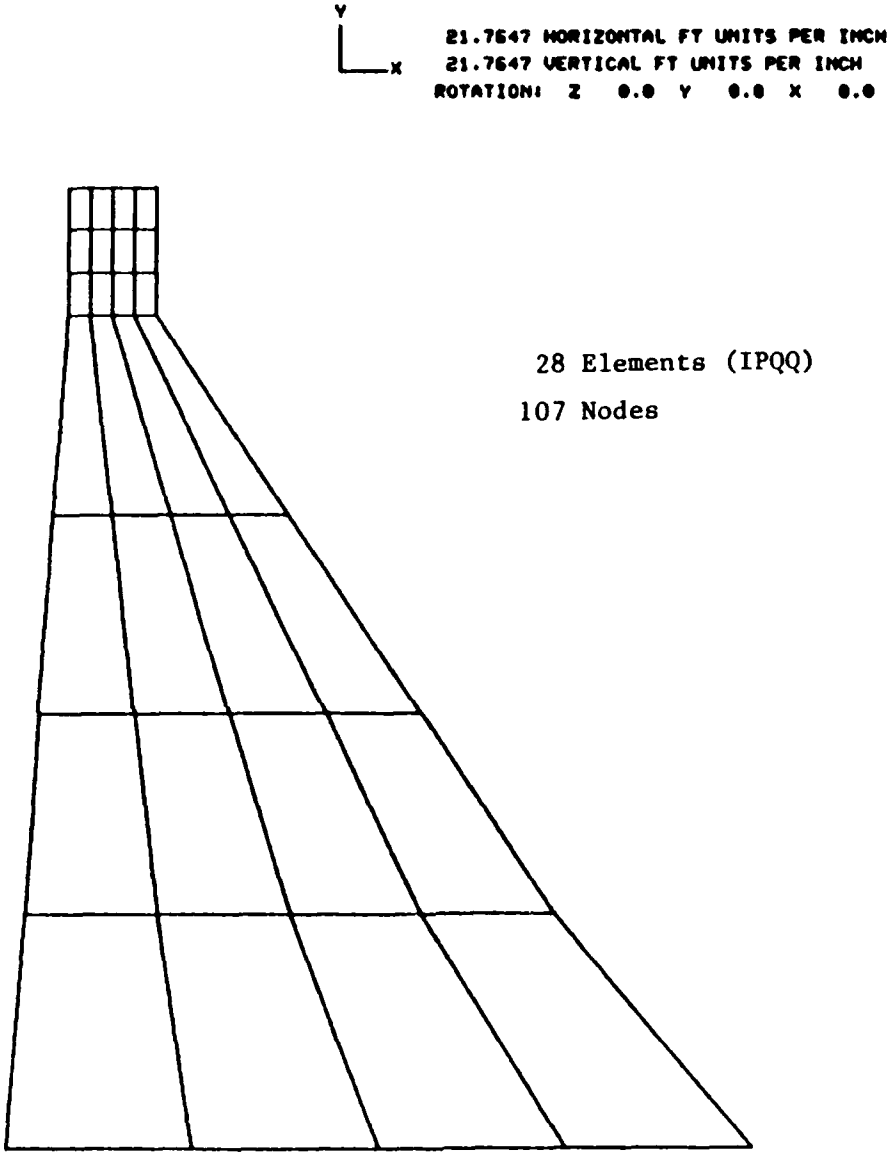

Figure 15. Mesh RBR4 for dam monolith

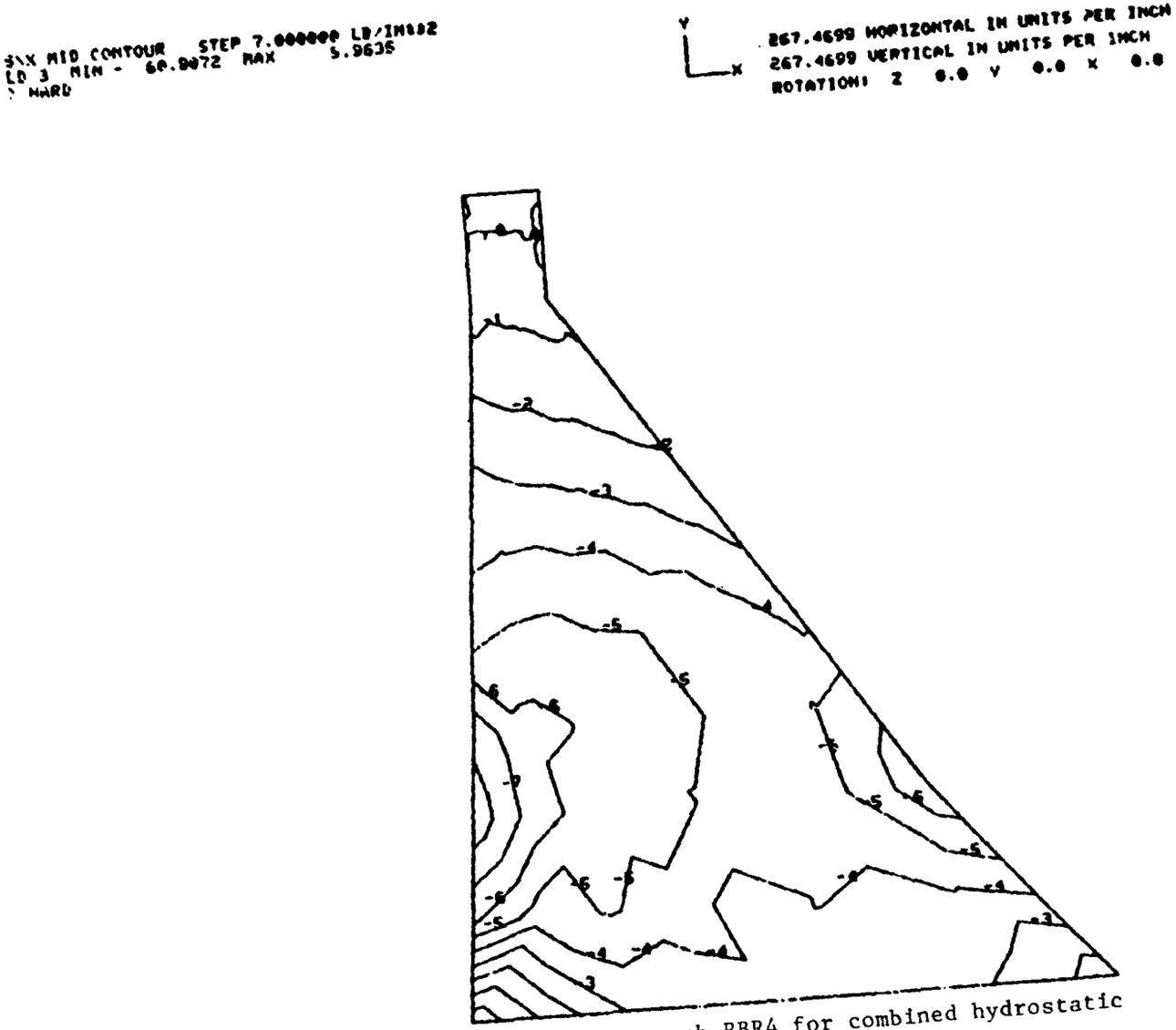

Figure 16. SXX contour plot for mesh RBR4 for combined hydrostatic plus body-force loading

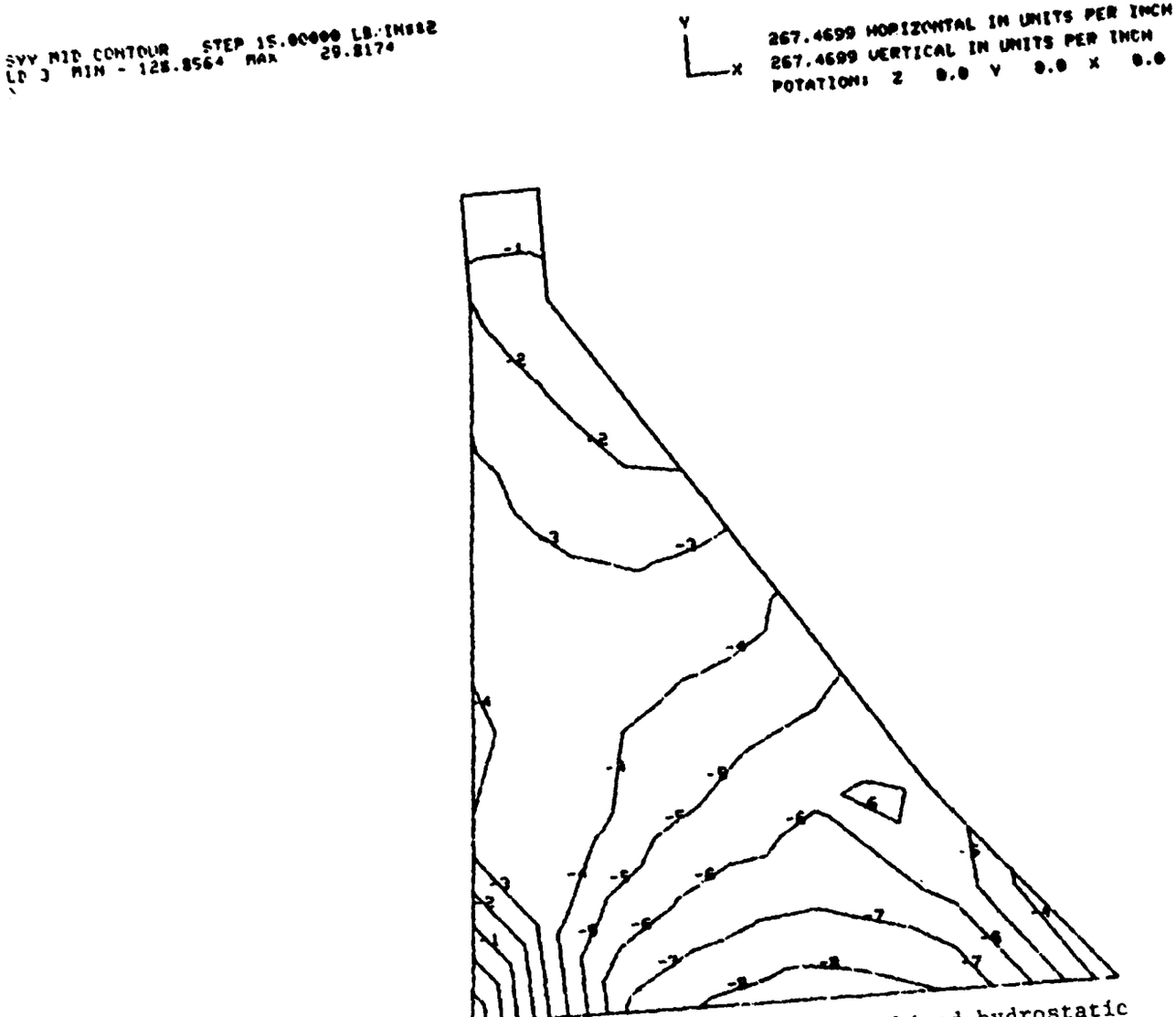

Figure 17. SYY contour plot for mesh RBR4 for combined hydrostatic plus body-force loading

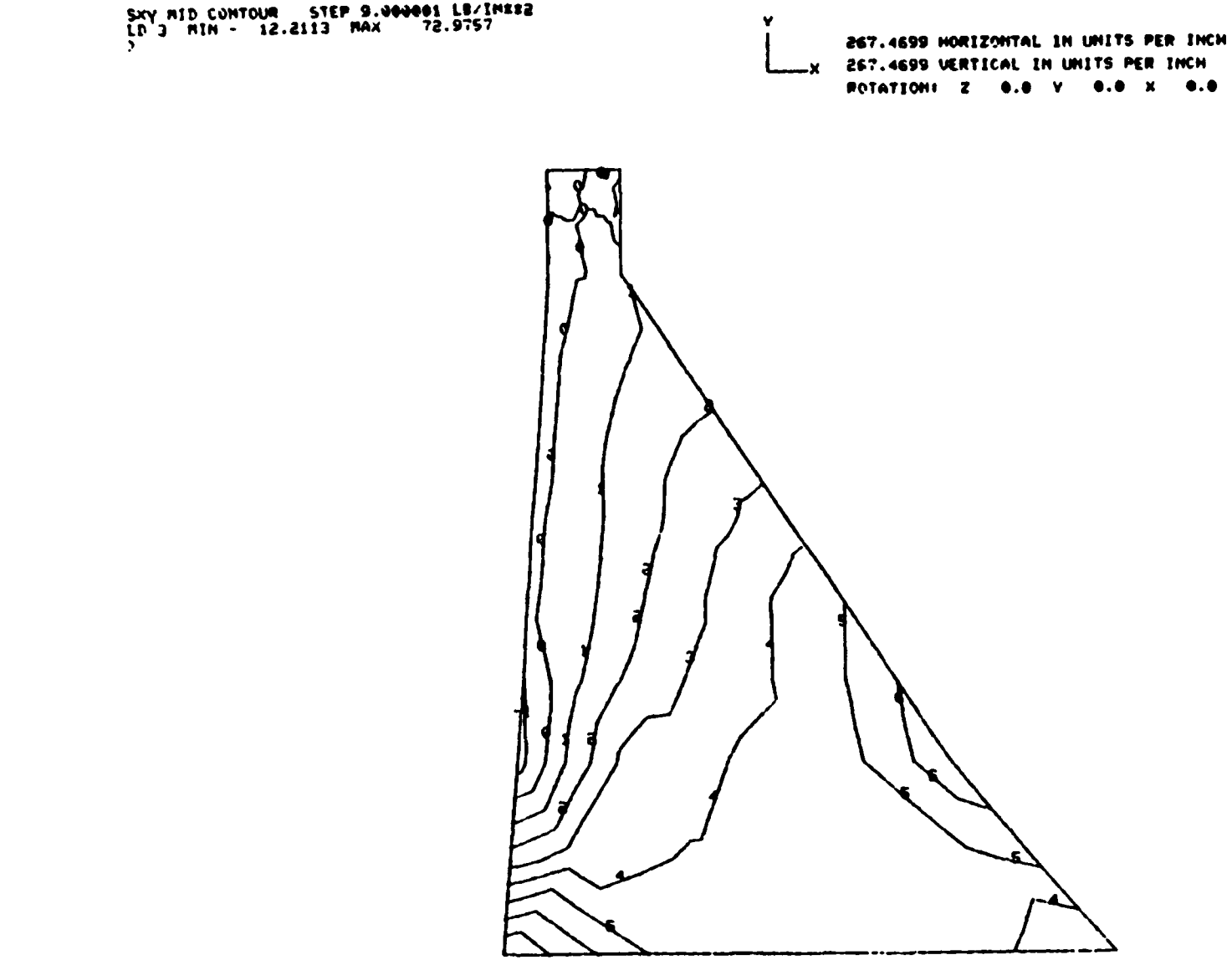

Figure 18. SXY contour plot for mesh RBR4 for combined hydrostatic plus body-force loading

41. The engineer then faces the question of accuracy of the solution. For mesh RBR4, one indication that the mesh was not fine enough was the sharp changes in the lines on the stress contour plots in Figures 16 through 18. These changes indicate that the stresses in these areas are changing rapidly and a finer mesh is required.

42. The next step was to refine the mesh. Six elements were used along the base with finer subdivisions in the vertical direction. This mesh, mesh RBR6, is shown in Figure 19. This mesh was also graded to facilitate automatic generation, although the tapered sides were accurately represented. Mesh RBR6 contained 102 elements and 353 nodes. Therefore, it was a considerably finer mesh than mesh RBR4.

43. Mesh RBR6 was analyzed for the combined effects of hydrostatic and body-force loading. Contour plots were obtained for the SXX, SYY, and SXY stress components and are shown in Figures 20 through 22, respectively. The contour plots produced much smoother curves, although the contour lines near the heel of the monolith did indicate that the stresses were changing rapidly in that area. Thus, a finer mesh would be required to accurately predict the stresses near the heel. The difficult question facing the engineer in the convergence of the results is: Are the results accurate? Comparing the results of meshes RBR4 and RBR6 indicated that the range of the stress components had changed considerably between meshes RBR4 and RBR6. For instance, in mesh RBR4 the maximum SXX stress was 5.96 psi while in mesh RBR6 the maximum SXX stress was 19.52 psi. Overlaying the contour plots for the various components also revealed that the contours were quite different in shape and magnitude except near the top of the monolith which was a lowly stressed region. Based on these comparisons, the engineer may decide that a finer mesh is needed.

44. Since the model selected in Phase I was going to be used in further foundation and dynamic analysis studies, the decision was made to further refine the mesh to one with eight elements across the base and more elements in the vertical direction. This mesh, mesh RBR8, is shown in Figure 23 and contained 192 elements and 641 nodes. Mesh RBR8 was also analyzed for the combined effect of hydrostatic and body force loadings. The results were analyzed using contour plots, and the SXX, SYY, and SXY contours are presented in Figures 24, 25, and 26, respectively. Comparing the contour plots for mesh RBR8 with those of mesh RBR6 (Figures 20, 21, and 22) indicated that

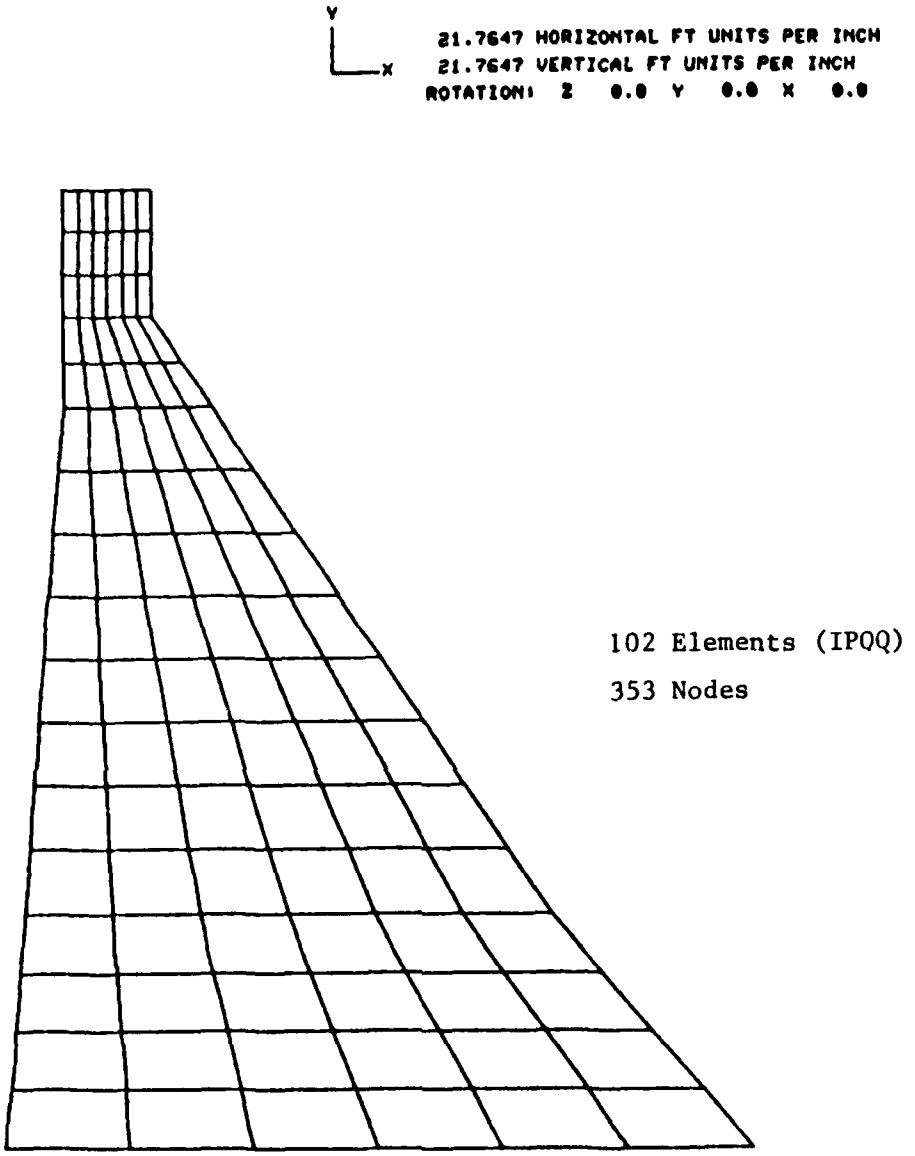

Figure 19. Mesh RBR6 for dam monolith

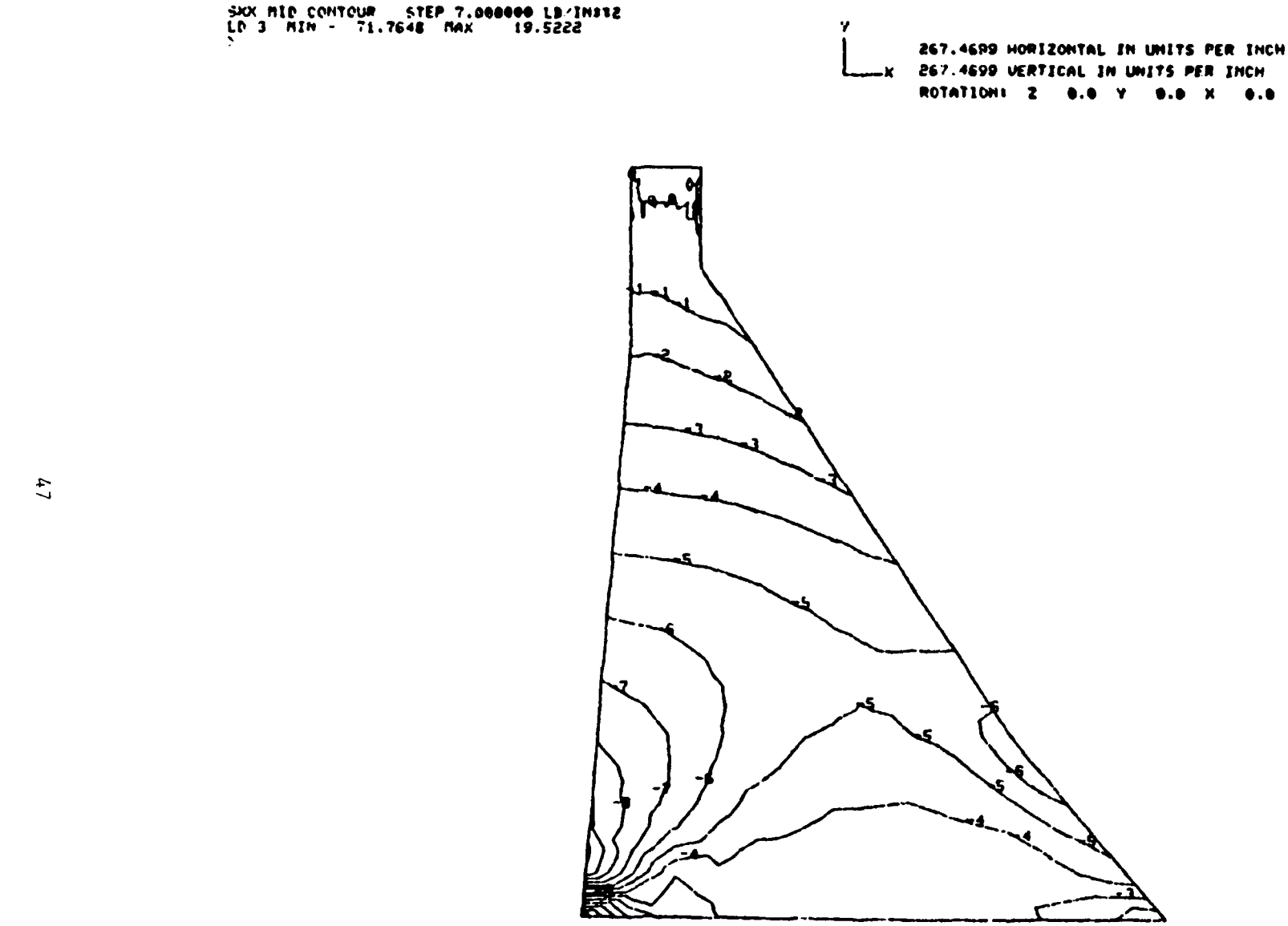

Figure 20. SXX contour plot for mesh RBR6 for combined hydrostatic plus body-force loading

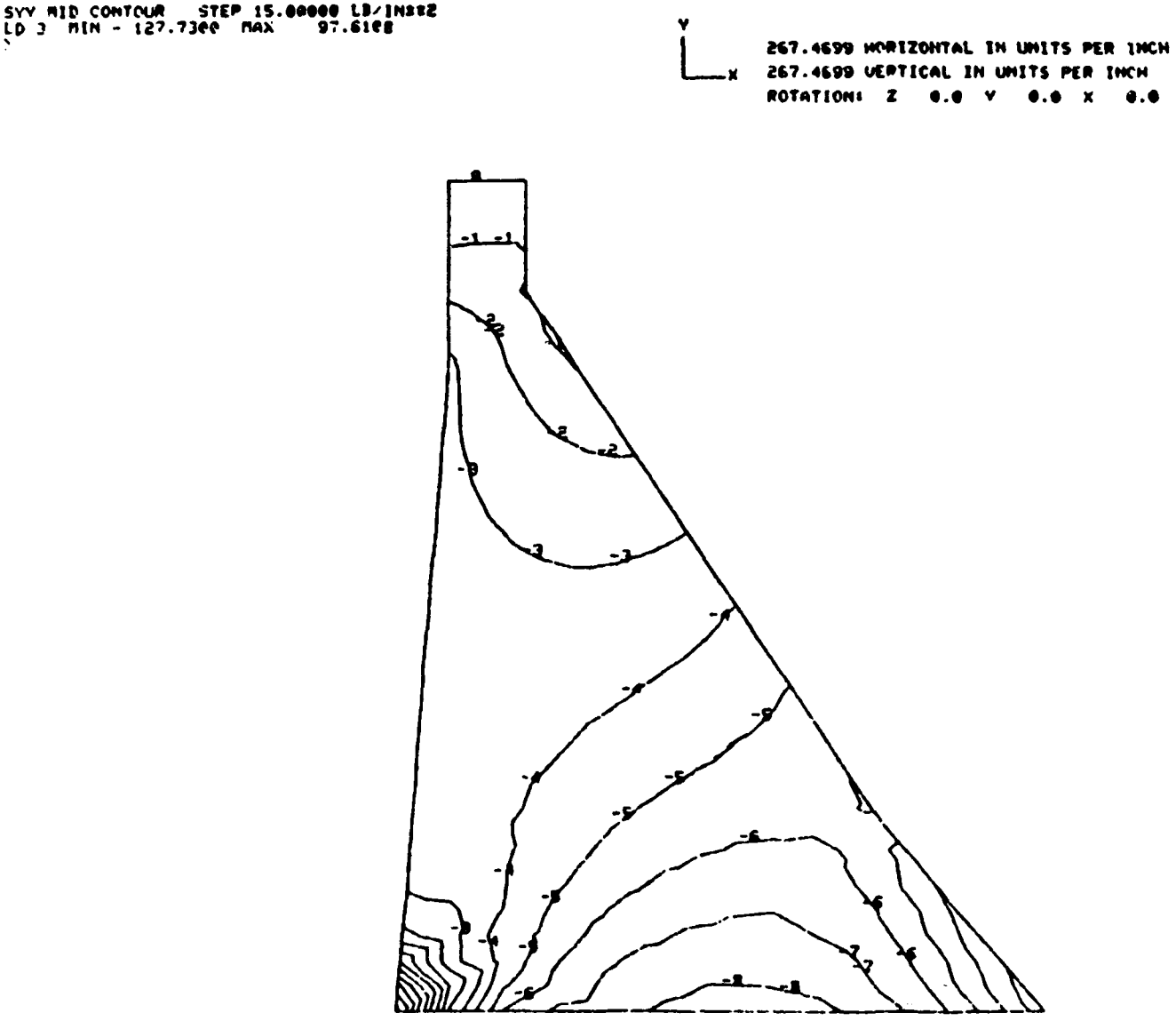

Figure 21. SYY contour plot for mesh RBR6 for combined hydrostatic plus body-force loading

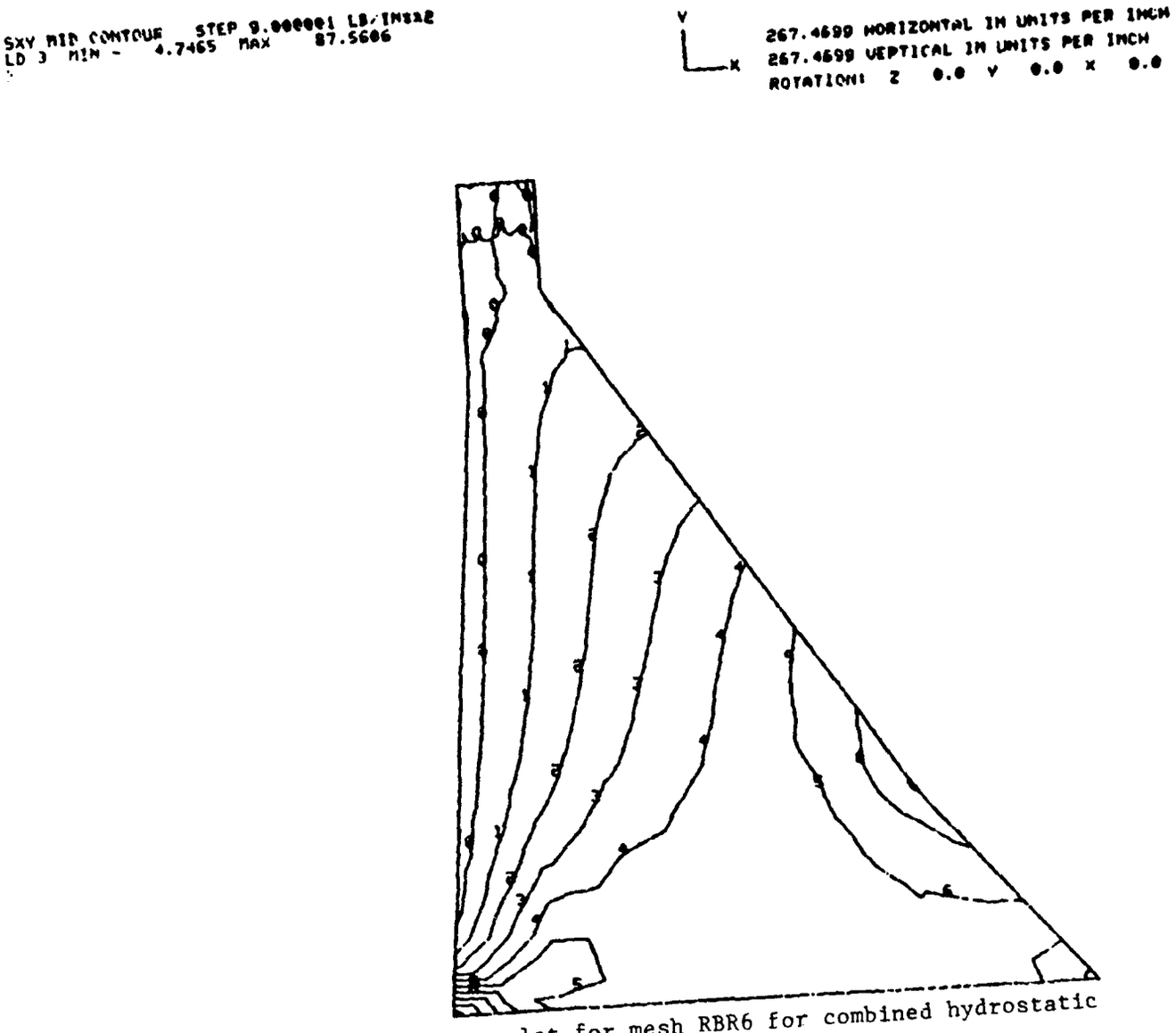

Figure 22. SXY contour plot for mesh RBR6 for combined hydrostatic plus body-force loading

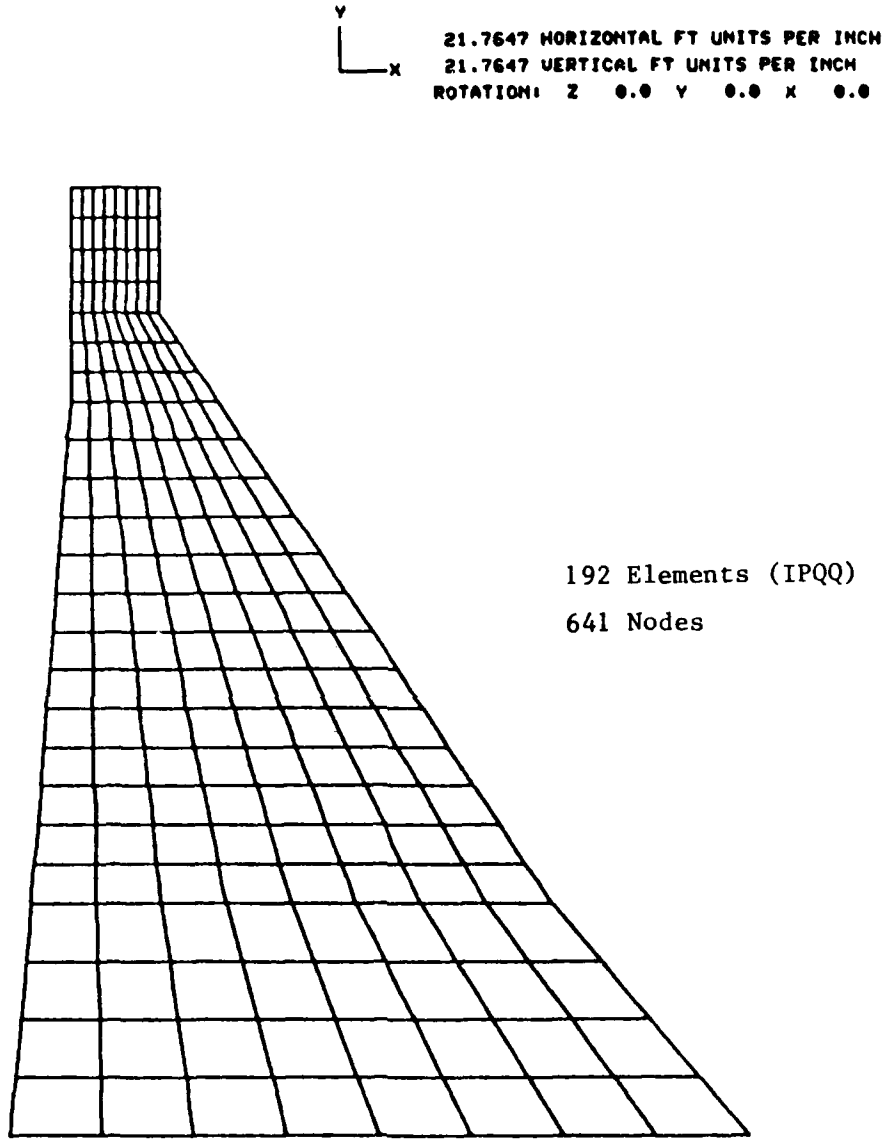

Figure 23. Mesh RBR8 for dam monolith

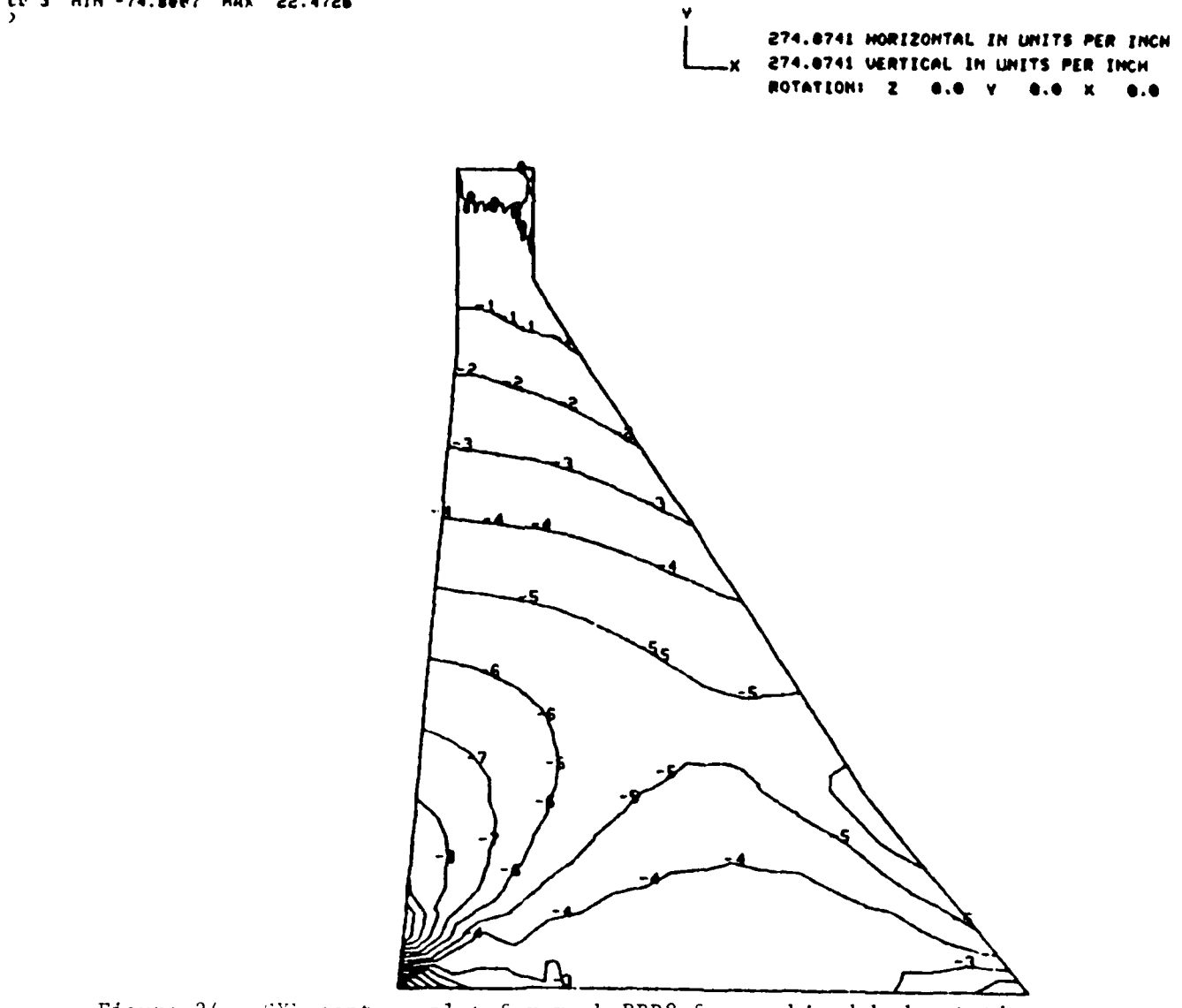

Figure 24. SXX contour plot for mesh RBR8 for combined hydrostatic plus body-force loading

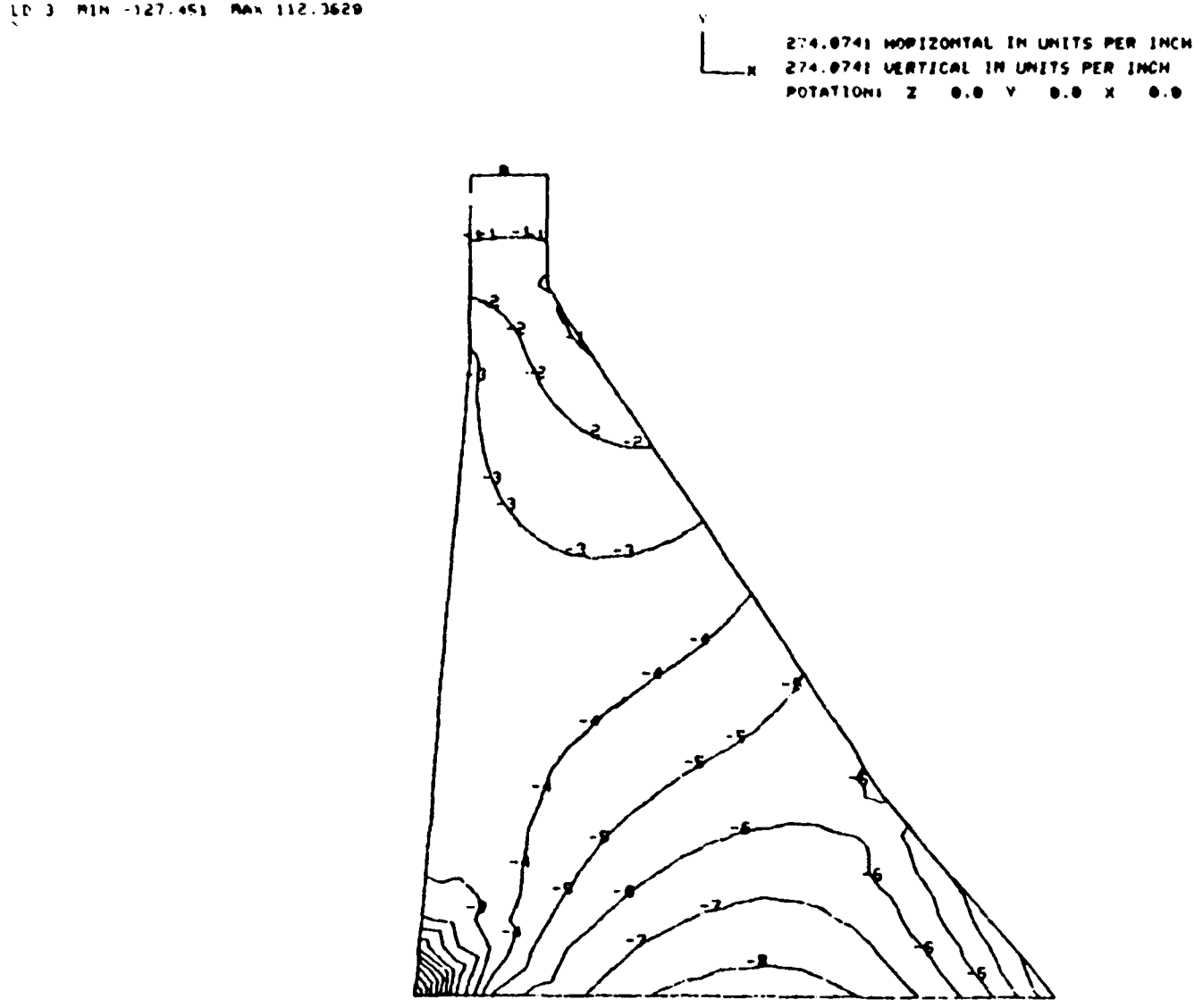

Figure 25. SYY contour plot for mesh RBR8 for combined hydrostatic plus body-force loading

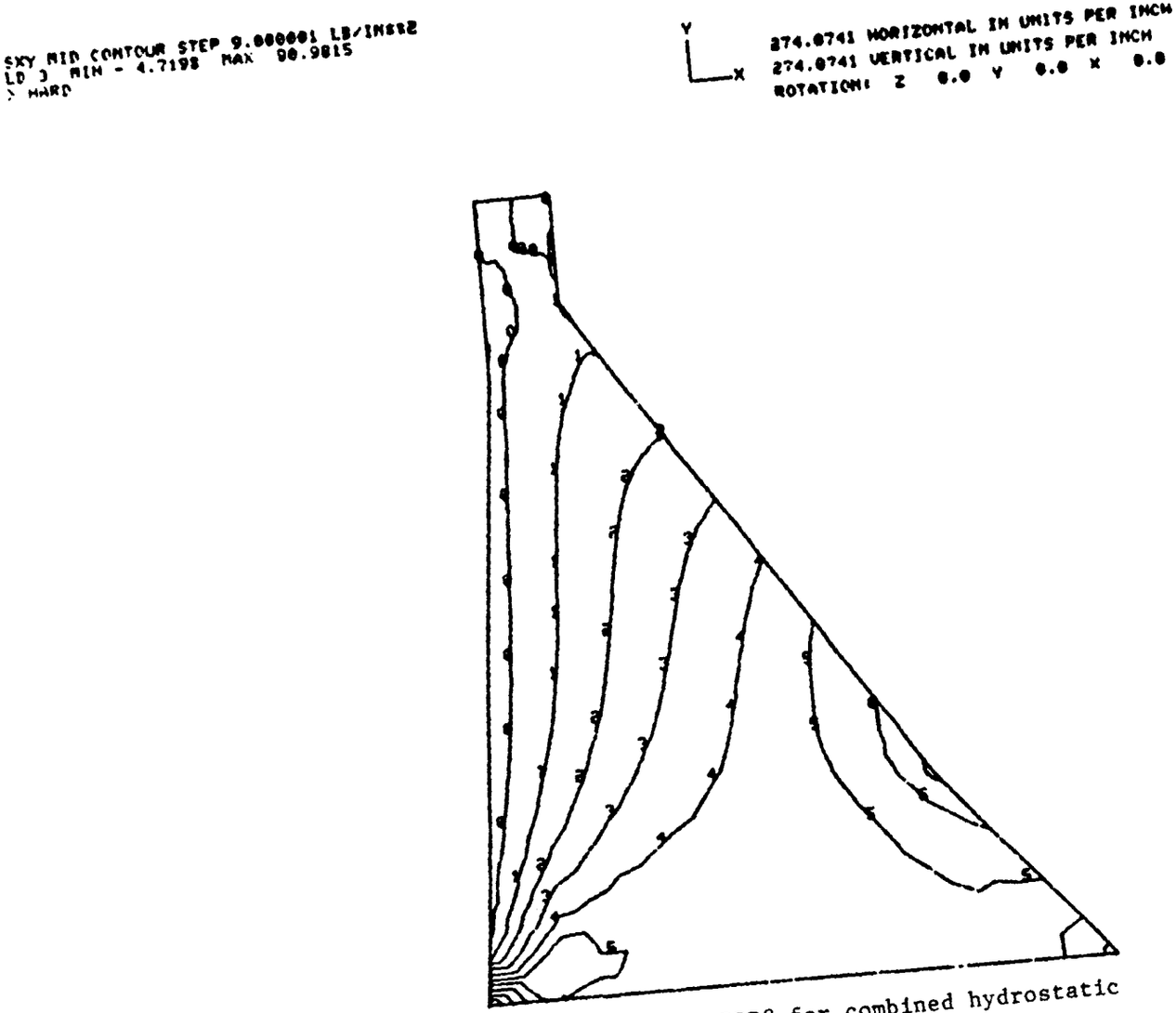

Figure 26. SXY contour plot for mesh RBR8 for combined hydrostatic plus body-force loading

there was very little change in the magnitude or distribution of the stresses except near the stress concentration at the heel of the monolith for all meshes. Table 12 summarizes the minimum and maximum stress components for meshes RBR4, RBR6, and RBR8. The following points should be noted from the results in Table 12:

a. The results for mesh RBR6 are close to those of mesh RBR8. The contour plots reveal that the major differences were isolated at the heel of the monolith.

b. The results for the coarsest mesh, mesh RBR4, were not conservative and if used, could lead to design errors.

Table 12

Comparison of Minimum and Maximum Stresses* for Meshes RBR4, RBR6, and RBR8

	RBR4	RBR6	RBR8
SXX min	-60.91	-71.76	-74.80
SXX max	5.96	19.52	22.47
SYY min	-128.85	-127.73	-127.45
SYY max	29.82	97.61	112.36
SXY min	-12.21	-4.75	-4.72
SXY max	72.98	87.56	90.98

* All measurements are in psi.

45. Based on these observations and the contour plots, mesh RBR6 was selected as adequate for use in further studies. The primary criterion for selecting mesh RBR6 over mesh RBR8 was that the RBR6 mesh provided acceptable accuracy for a lower computational cost. Mesh RBR6 contained 102 elements and 353 nodes while mesh RBR8 contained 192 elements and 641 nodes. A listing of the input data required for mesh RBR6 is presented in Appendix C.

Plane Strain Versus Plane Stress

46. The models analyzed in paragraphs 40 through 45 were assumed to be in a state of plane stress. When modeling a three-dimensional structure using a two-dimensional model, an initial decision is the type analysis to be

performed. For this study, a plane strain and a plane stress analysis were the choices.

47. In order to assess the effect of the plane stress versus plane strain assumption, mesh RBR6 was analyzed, assuming plane strain as well as stress. Contour plots were again obtained and are shown in Figures 27, 28, and 29. Comparison of these three figures with those of RBR6 under plane stress, Figures 20, 21, and 22, indicated that although the minimum and maximum stress components did change, the change was relatively minor. Also, the distribution of the stress was essentially the same with minor changes only in the SXX and SXY stress components near the center of the base.

Effect of Gallery on Overall Behavior

48. In the analyses presented in the previous paragraphs, a gallery located near the heel of the monolith was ignored. In order to assess the effect of the gallery on the overall behavior of the model, mesh RBR6 was modified to account for the gallery. Since the emphasis in this analysis was to evaluate the overall behavior and not to determine a detailed understanding of the state of stress near the gallery, mesh RBR6 was modified to account for the hole as shown in Figure 30. If a more accurate representation of the state of stress was needed near the gallery area, a much finer mesh would be required in that area with a transition zone to the regular mesh also needed.

49. Mesh RBR6 was assumed to be in a state of plane stress and was analyzed for the combined effects of hydrostatic and body-force loading. Stress contour plots were obtained and are presented in Figures 31, 32, and 33. These plots revealed that while the maximum and minimum stresses changed considerably, most of the changes were in the area of the heel due to the combined effects of the stress concentration at the heel and the gallery area.

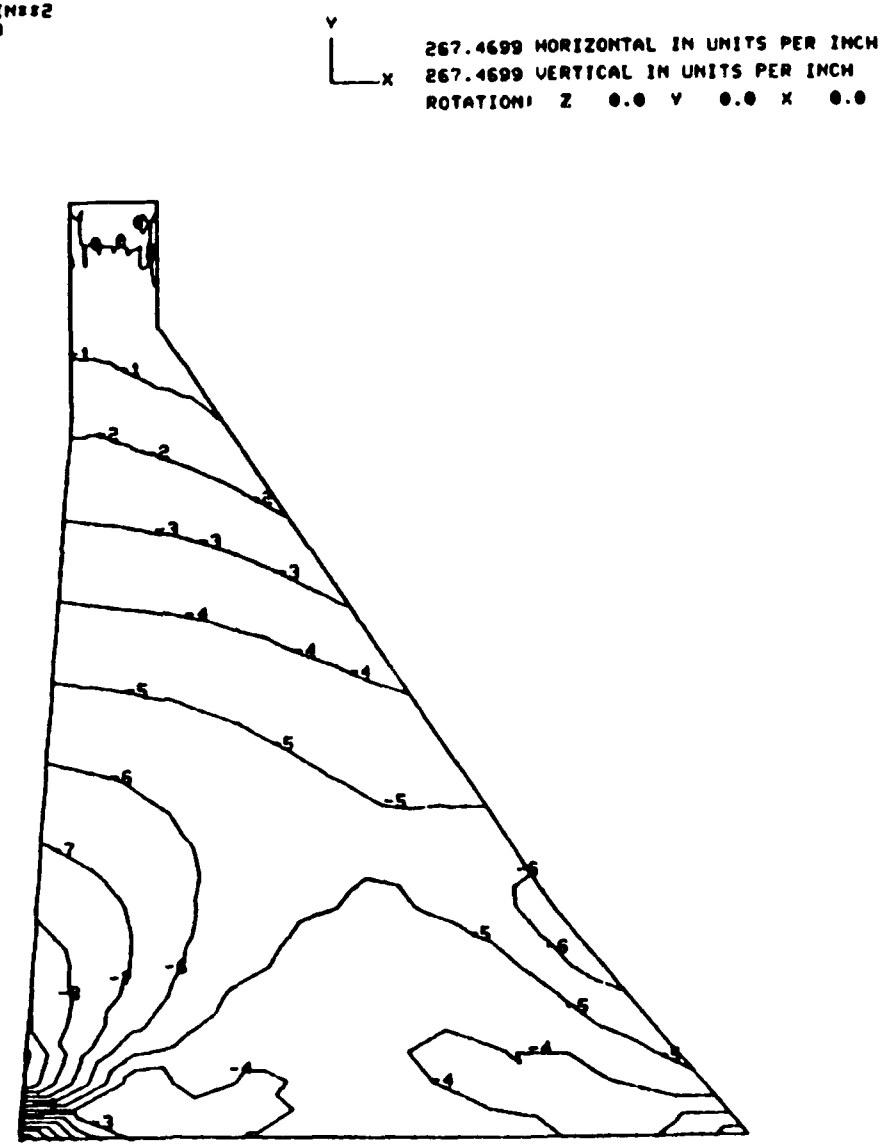

Figure 27. SXX contour plot for mesh RBR6 under plane strain for combined hydrostatic and body-force loading

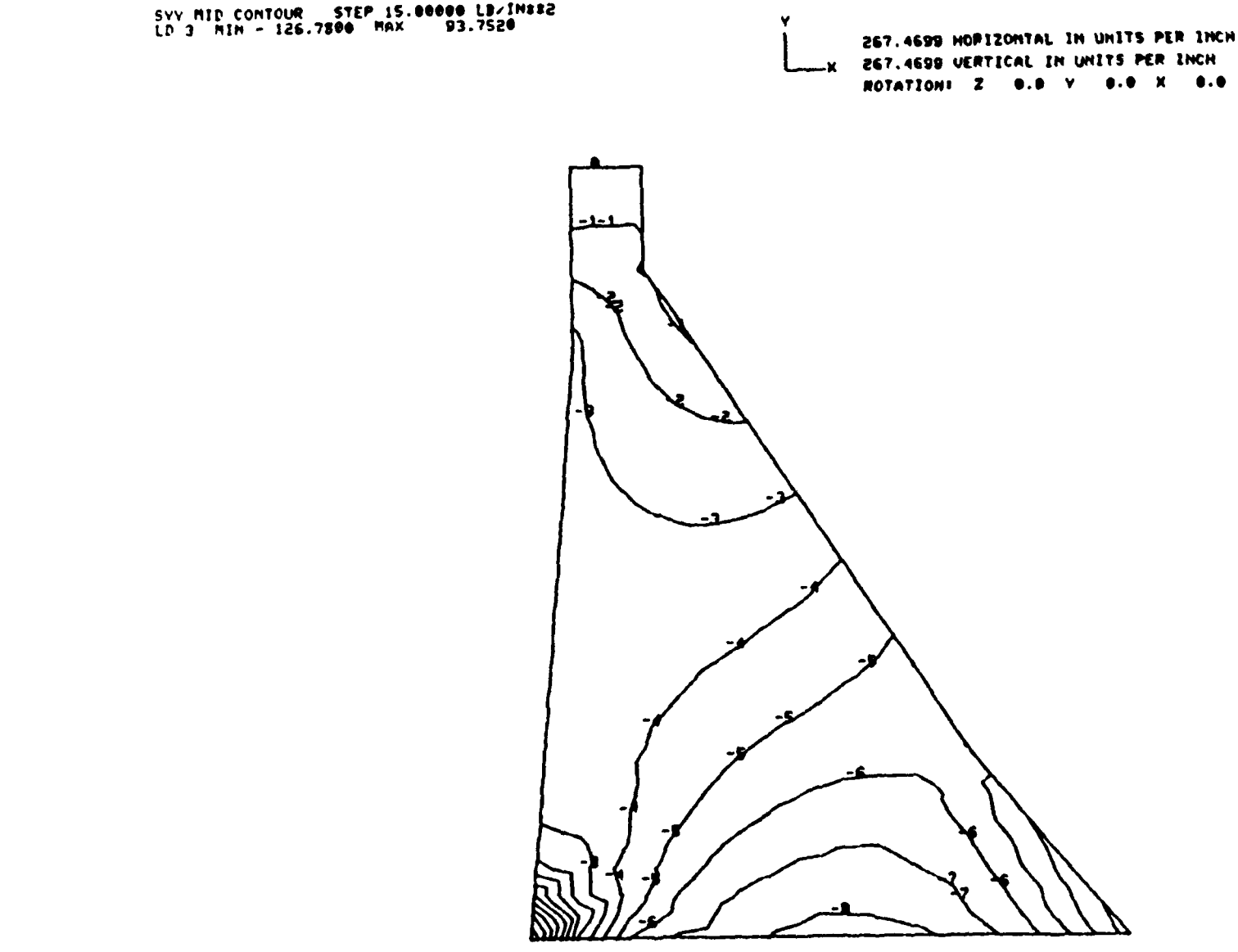

Figure 28. SYY contour plot for mesh RBR6 under plane strain for combined hydrostatic and body-force loading

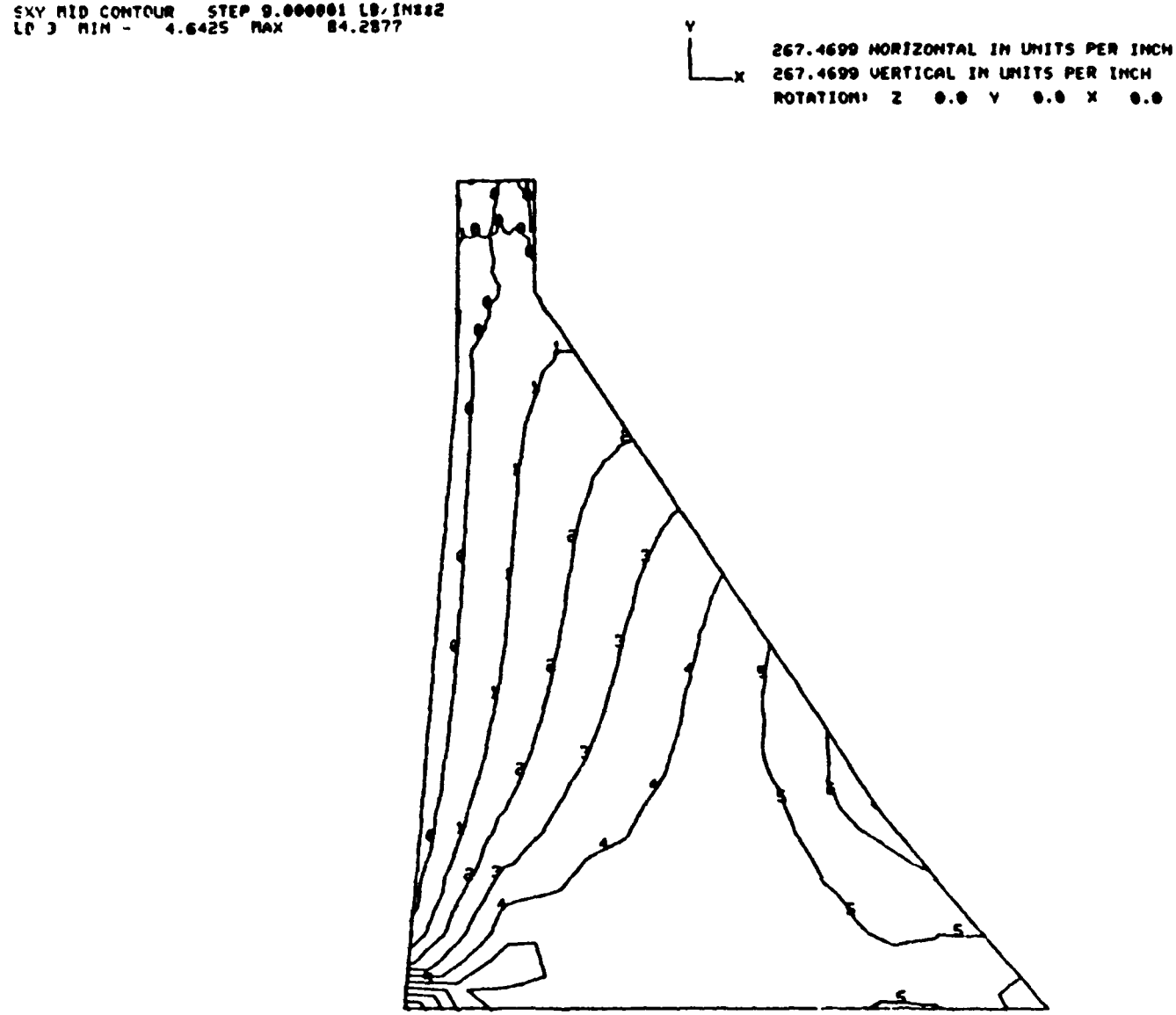

Figure 29. SXY contour plot for mesh RBR6 under plane strain for combined hydrostatic and body-force loading

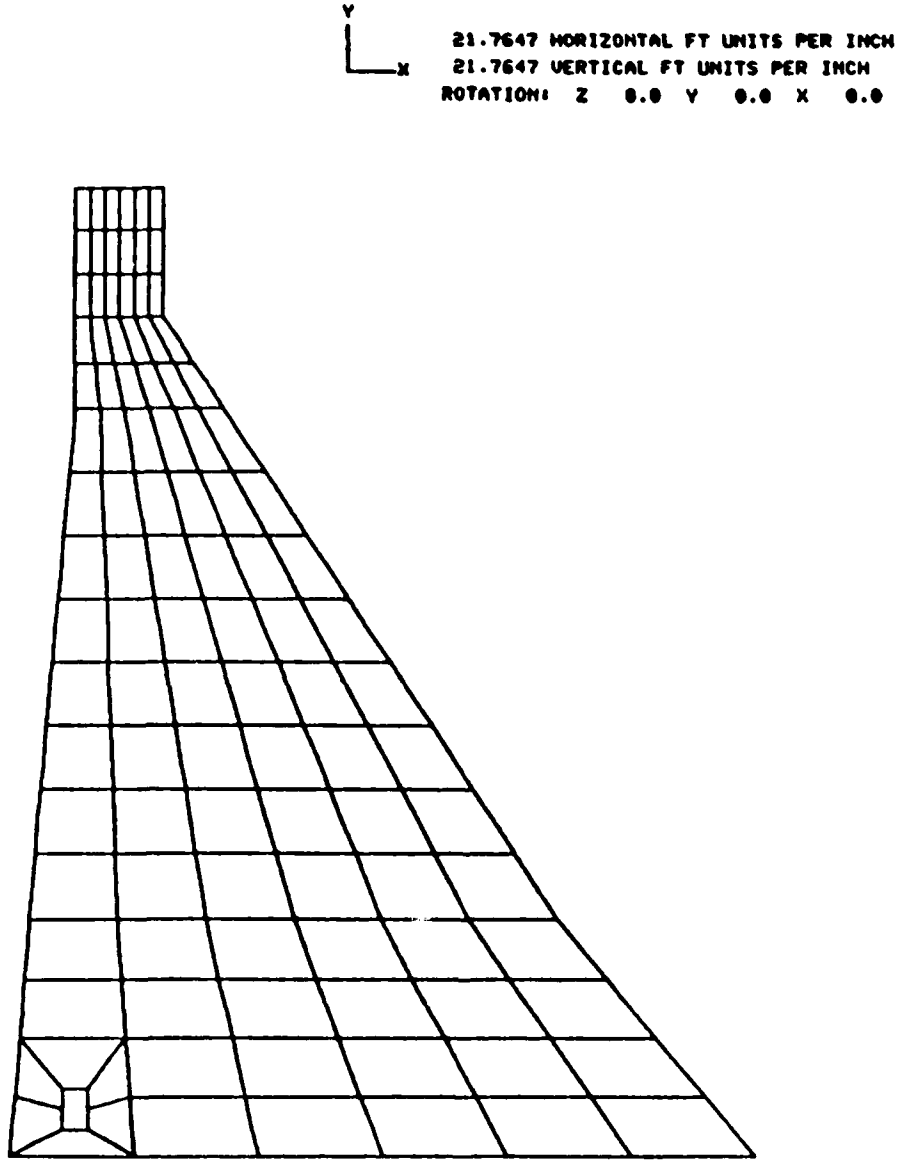

Figure 30. Mesh RBR6 with gallery

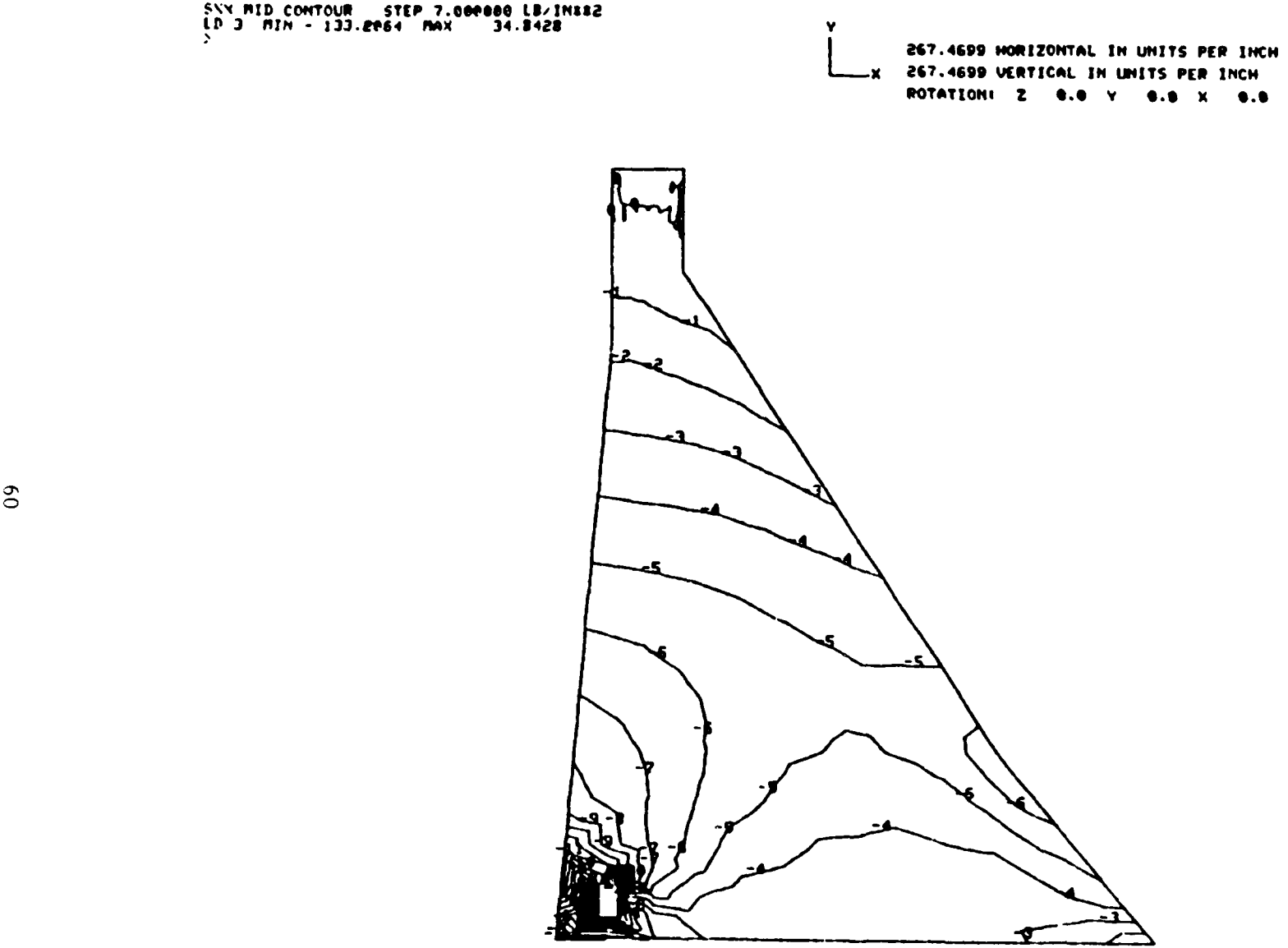

Figure 31. SXX contour plot for mesh RBR6 with gallery due to combined hydrostatic and body-force loading

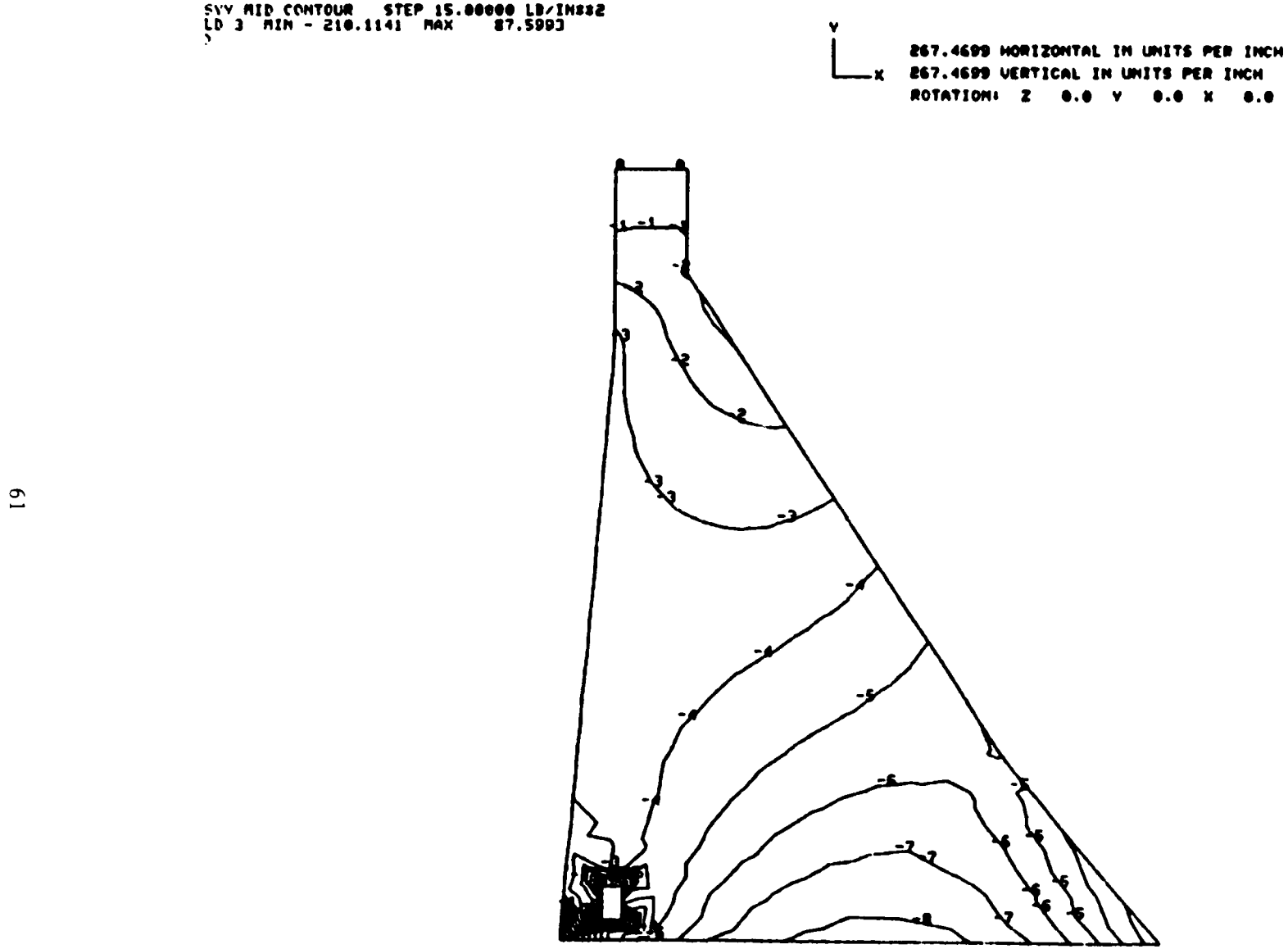

Figure 32. SYY contour plot for mesh RBR6 with gallery due to combined hydrostatic and body-force loading

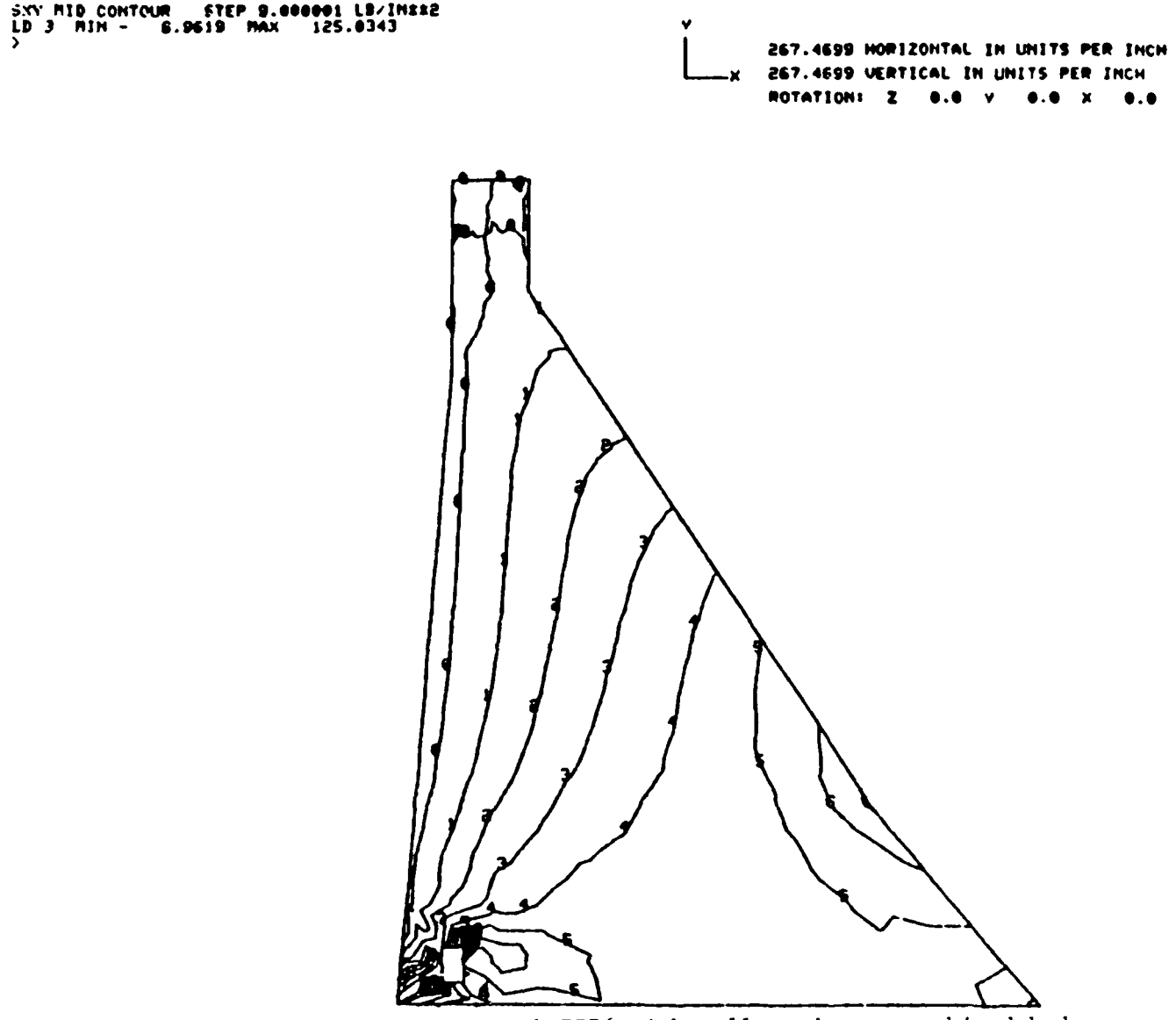

Figure 33. SXY contour plot for mesh RBR6 with gallery due to combined hydrostatic and body-force loading

PART IV: SUMMARY

50. The primary objective of this study was to illustrate an approach for performing a static finite element analysis of a Corps structure, the monolith of a dam. The illustration served two purposes:

a. To aid the beginning finite element analyst with an understanding of the necessary steps for performing a finite element analysis.

b. To develop an understanding of the behavior of a gravity dam.

51. The analyses of a monolith of the RBR Dam determined that a mesh with six elements across the base, mesh RBR6, yielded satisfactory results for the overall behavior of the structure. The gallery was found to have little effect on the overall behavior but greatly affected the state of stress in the vicinity of the gallery due to the combined effects of the stress concentration near the heel and the gallery area. The assumption of plane stress or plane strain had little effect on the results. In conclusion, RBR6, is recommended for future foundation and dynamic analysis studies to be performed in subsequent phases of this study.

APPENDIX A: MESH 2 FOR CASES A1, A2, B1, AND B2

```
*TITLE 'CASE A CANTILEVER FINE MESH - MESH B'
STRUDL 'CASE A' 'CANTILEVER FINE MESH - MESH B'
$
UNITS FEET LBS
TYPE PLANE STRESS
$
$     GENERATE ALL NODES HAVING ZERO COORDINATES
$     AND THEN CHANGE CORNER NODES TO CORRECT VALUES.
$     THIS WILL WORK SINCE GTSTRUDL WILL AUTOMATICALLY
$     COMPUTE THE CORRECT COORDINATES FOR THE MID-SIDE
$     NODES IF THE MID-SIDE NODES HAVE COORDINATES OF
$     0,0,0.  GTSTRUDL WILL THEN ASSUME THAT THE COORDINATES
$     ARE HALF-WAY ALONG THE EDGE WHICH IS THE CORRECT
$     POSITION FOR THIS PROBLEM.
$
GENERATE 149 JOI ID 1 1 X 0 0 Y 0 0 Z 0 0
$
$     ENTER CHANGES MODE TO GENERATE THE CORRECT COORDINATES
$     FOR THE CORNER NODES.
$
CHANGES
$
JOINT COORDINATES
1 0.0 0.0
9 80.0 0.0
141 0.0 185.0
149 80.0 185.0
$
GENERATE BETWEEN 1 9 149 141
XDIRECTION 4 PARTS EQUAL
YDIRECTION 10 PARTS EQUAL
$
ADDITIONS
$
GENERATE 4 ELEMENTS ID 1 1 F 1 2 T 3 2 T 17 2 T 15 2 T 2 2 T 11 1 T 16 2 T 10 1
REPEAT 9 ID 4 F 14
$
STATUS SUPPORT 1 TO 9
JOINT RELEASES
1 TO 4 6 TO 9 FORCE X
$
ELEMENT PROPERTIES
1 TO 40 TYPE 'IPQD' THICK 1.0
$
PLOT PROJECTION
$
CONSTANTS
E 576000000.
POISSON 0.2
$
$
UNITS KIPS
LOADING 1 'HORIZONTAL FORCE AT TOP'
$
$     TRIBUTARY AREA USED TO DISTRIBUTE FORCE AT NODES 141-149
$
JOINT LOADS
141 149    FORCE X 62.5
142 TO 148 FORCE X 125.0
```

Figure A1. Input for mesh 2, Cases A1 and A2 (Continued)

```
$
$
$
UNITS LBS
LOADING 2  LINEAR DISTRIBUTED HORIZONTAL LOAD'
$
ELEMENT LOAD
$
$
39 EDGE FORCE EDGE 4 GLOBAL VARIABLE VX     0.0   577.2  1154.4
35 EDGE FORCE EDGE 4 GLOBAL VARIABLE VX  1154.4  1731.6  2308.8
31 EDGE FORCE EDGE 4 GLOBAL VARIABLE VX  2308.8  2886.0  3463.2
27 EDGE FORCE EDGE 4 GLOBAL VARIABLE VX  3463.2  4040.4  4617.6
23 EDGE FORCE EDGE 4 GLOBAL VARIABLE VX  4617.6  5194.8  5772.0
19 EDGE FORCE EDGE 4 GLOBAL VARIABLE VX  5772.0  6349.2  6926.4
15 EDGE FORCE EDGE 4 GLOBAL VARIABLE VX  6926.4  7503.6  8080.8
11 EDGE FORCE EDGE 4 GLOBAL VARIABLE VX  8080.8  8658.0  9235.2
7  EDGE FORCE EDGE 4 GLOBAL VARIABLE VX  9235.2  9812.4 10389.6
3  EDGE FORCE EDGE 4 GLOBAL VARIABLE VX 10389.6 10966.8 11544.0
$
$
STIFFNESS ANALYSIS
$
LIST DISP
$
LIST REACTIONS
$
LIST SUM REACTIONS
$
LIST STRESSES
$
CALCULATE AVERAGE STRESSES
$
SAVE 'CASEAF'
FINISH
```

Figure A1. (Concluded)

```
*TITLE  CASE B  CANTILEVER FINE MESH - MESH 2'
STRUDL  CASE B   'CANTILEVER FINE MESH - MESH 2'
$
UNITS FEET LBS
TYPE PLANE STRESS
$
$     GENERATE ALL NODES HAVING ZERO COORDINATES
$     AND THEN CHANGE CORNER NODES TO CORRECT VALUES.
$     THIS WILL WORK SINCE GTSTRUDL WILL AUTOMATICALLY
$     COMPUTE THE CORRECT COORDINATES FOR THE MID-SIDE
$     NODES IF THE MID-SIDE NODES HAVE COORDINATES OF
$     0,0,0.  GTSTRUDL WILL THEN ASSUME THAT THE COORDINATES
$     ARE HALF-WAY ALONG THE EDGE WHICH IS THE CORRECT
$     POSITION FOR THIS PROBLEM.
$
GENERATE 149 JOI ID 1 1 X 0 0 Y 0 0 Z 0 0
$
$     ENTER CHANGES MODE TO GENERATE THE CORRECT COORDINATES
$     FOR THE CORNER NODES.
$
CHANGES
$
JOINT COORDINATES
1 0.0 0.0
9 143.25 0.0
141 63.125 185.0
149 80.125 185.0
$
GENERATE BETWEEN 1 9 149 141
XDIRECTION 4 PARTS EQUAL
YDIRECTION 10 PARTS EQUAL
$
ADDITIONS
$
GENERATE 4 ELEMENTS ID 1 1 F 1 2 T 3 2 T 17 2 T 15 2 T 2 2 T 11 1 T 16 2 T 10
REPEAT 9 ID 4 F 14
$
STATUS SUPPORT 1 TO 9
JOINT RELEASES
1 TO 4 6 TO 9 FORCE X
$
ELEMENT PROPERTIES
1 TO 40 TYPE  IP00' THICK 1.0
$
PLOT PROJECTION
$
CONSTANTS
E 576000000.
POISSON 0.2
$
$
UNITS KIPS
LOADING 1  HORIZONTAL FORCE AT TOP'
$
$     TRIBUTARY AREA USED TO DISTRIBUTE FORCE AT NODES 141-149
$
JOINT LOADS
141 149    FORCE X 62.5
142 TO 148 FORCE X 125.0
```

Figure A2. Input for mesh 2, Cases B1 and B2 (Continued)

```
$
$
$
$
$
UNITS LBS
LOADING 2 'LINEAR DISTRIBUTED HORIZONTAL LOAD'
$
ELEMENT LOAD
$
$
39 EDGE FORCE EDGE 4 GLOBAL VARIABLE VX     0.0   577.2  1154.4
35 EDGE FORCE EDGE 4 GLOBAL VARIABLE VX  1154.4  1731.6  2308.8
31 EDGE FORCE EDGE 4 GLOBAL VARIABLE VX  2308.8  2886.0  3463.2
27 EDGE FORCE EDGE 4 GLOBAL VARIABLE VX  3463.2  4040.4  4617.6
23 EDGE FORCE EDGE 4 GLOBAL VARIABLE VX  4617.6  5194.8  5772.0
19 EDGE FORCE EDGE 4 GLOBAL VARIABLE VX  5772.0  6349.2  6926.4
15 EDGE FORCE EDGE 4 GLOBAL VARIABLE VX  6926.4  7503.6  8080.8
11 EDGE FORCE EDGE 4 GLOBAL VARIABLE VX  8080.8  8658.0  9235.2
7  EDGE FORCE EDGE 4 GLOBAL VARIABLE VX  9235.2  9812.4 10389.6
3  EDGE FORCE EDGE 4 GLOBAL VARIABLE VX 10389.6 10966.8 11544.0
$
$
STIFFNESS ANALYSIS
$
LIST DISP
$
LIST REACTIONS
$
LIST SUM REACTIONS
$
LIST STRESSES
$
CALCULATE AVERAGE STRESSES
$
SAVE 'CASEBF'
FINISH
```

Figure A2. (Concluded)

APPENDIX B: TIMOSHENKO BEAM THEORY AND THEORY OF ELASTICITY SOLUTIONS FOR SIMPLIFIED MODELS--CASES A1, A2, AND B1

Case A1*

Deflection Curve

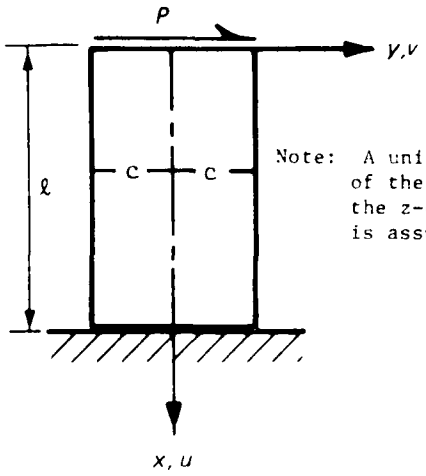

Note: A unit thickness of the beam in the z-direction is assumed.

$$v^{tb} = \frac{P(\ell - x)^2}{6EI}(2\ell - x) + \frac{P(\ell - x)}{KGA}$$

$$K = \frac{10(1 + \nu)}{12 + 11\nu}$$

$$v^{af} = \frac{Px^3}{6EI} - \frac{P\ell^2 x}{2EI} + \frac{P\ell^3}{3EI} + \frac{Pc^2}{2GI}(\ell - x)$$

G = modulus of elasticity in shear

E = modulus of elasticity in tension and compression

I = moment of inertia of a cross section of the beam

ℓ = length of beam

ν = Poisson's ratio

P = load applied to end of beam

A = cross-sectional area

Stress

$$\sigma_{xx}^{tb} = \sigma_{xx}^{af} = \frac{My}{I}$$

$$\sigma_{xy}^{tb} = \sigma_{xy}^{af} = \frac{VQ}{(1)I}$$

where

tb: Timoshenko Beam
af: Airy Stress Function (Theory of Elasticity)

---

* S. P. Timoshenko and J. N. Goodier. 1951. Theory of Elasticity, McGraw-Hill, New York. This same reference applies for Cases A2 and B1.

Case A2

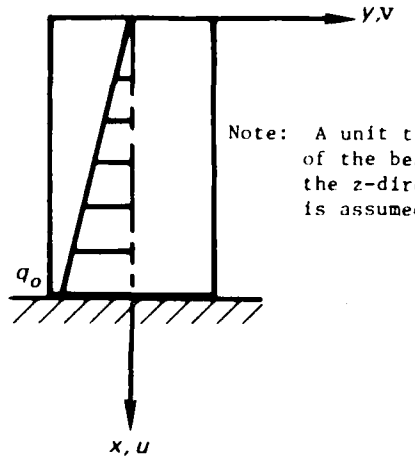

Note: A unit thickness of the beam in the z-direction is assumed.

Deflection Curve

$$v^{tb} = \frac{q_o(\ell - x)^2}{120EI\ell}(4\ell^3 + 2\ell x^2 + 3\ell^2 x + x^3)$$

$$+ \frac{q_o}{6KGA\ell}(\ell^3 - x^3)$$

$$v^{af} = \frac{1+\nu}{E}\left[xd + \frac{7q_o x^3}{30c} - \frac{\nu q_o x^3}{20c} + \frac{(\nu - 1)q_o x^5}{80c^3}\right] + h$$

$$d = \frac{-q_o c}{10} + (1 - \nu)\left(\frac{q_o \ell^4}{16c^3} + \frac{3q_o \ell^2}{20c}\right) + \frac{3\nu q_o \ell^2}{8c}$$

$$h = \frac{1+\nu}{E}\left[\frac{\nu q_o \ell^3}{20c} + \frac{(1 - \nu)q_o \ell^5}{80c^3} - \frac{7q_o \ell^3}{30c} - \ell d\right]$$

Stress

$$\sigma_{xx}^{tb} = \frac{My}{I}, \quad \sigma_{xy}^{tb} = \frac{VQ}{(1)I}$$

$$\sigma_{xx}^{af} = \frac{q_o x^3 y}{4c^3} + \frac{q_o}{4c^3}(-2xy^3 + \frac{6}{5}c^2 xy)$$

$$\sigma_{xy}^{af} = \frac{3q_o x^2}{8c^3}(c^2 - y^2) - \frac{q_o}{8c^3}(c^4 - y^4) + \frac{3q_o}{20c}(c^2 - y^2)$$

Case B1

Deflection Curve

$$v^{tb} = \ell n\left(\frac{h_1}{h_2 + \alpha x}\right)\left(\frac{P}{KGb\alpha} + \frac{12P}{\alpha^3 bE}\right)$$

$$+ \frac{6P(h_2 + 2h_1)(\ell - x)^2}{\alpha bE(h_2 + \alpha x)h_1^2}$$

$$- \frac{12P(\ell - x)}{\alpha^2 bE(h_2 + \alpha x)}$$

Note: Use b = 12 inches in the above equation

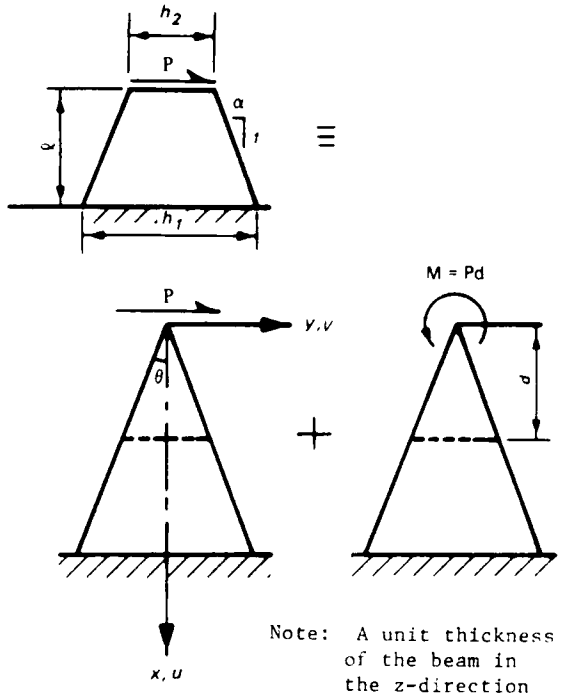

Note: A unit thickness of the beam in the z-direction is assumed.

Stress

$$\sigma_{xx}^{tb} = \frac{My}{I}, \qquad \sigma_{xy}^{tb} = \frac{VQ}{(1)I}$$

$$\sigma_{xx}^{af} = -\frac{FPyx^2}{(x^2 + y^2)^2} - \frac{RM}{x^2 + y^2}\left[\cos 2\alpha \frac{2xy}{x^2 + y^2} + \frac{2y^3x - 6yx^3}{(x^2 + y^2)^2}\right]$$

$$\sigma_{xy}^{af} = -\frac{FPxy^2}{(x^2 + y^2)^2} - \frac{RM}{x^2 + y^2}\left[\cos 2\alpha \frac{y^2 - x^2}{x^2 + y^2} + \frac{y^4 - 6x^2y^2 + x^4}{(x^2 + y^2)^2}\right]$$

$$F = \frac{2}{2\theta - \sin 2\theta}$$

$$R = \frac{1}{\sin 2\theta - 2\theta \cos 2\theta}$$

APPENDIX C: INPUT DATA FOR MESH RBR6

```
STRUDL 'RBRDAM6' 'RBR DAM MODEL WITH 6 ELEMENTS ACROSS BASE'
$
UNITS FT LBS
$
$    FIRST GENERATE ALL JOINTS AS HAVING ZERO COORDINATES AND THEN
$    GENERATE THE CORNER NODE COORDINATES FOR ALL ELEMENTS IN THE
$    CHANGES MODE.  GTSTRUDL WILL ASSUME THAT THE MIDSIDE NODES
$    ARE LOCATED HALF WAY BETWEEN THE CORNER NODES IF THE MIDSIDE NODES
$    HAVE COORDINATES OF ZERO.
$
GENE 353 JOI ID 1 1 X 0 0
$
$
CHANGES
$
$    CONTROLLING POINTS FOR GENERATE BETWEEN COMMANDS
$
JOINT COORDINATES
1
13 143.25
81 3.8333 46
93 104.917 46
241 11.916 143
253 40.249 143
281 11.916 160
293 28.916 160
341 11.916 185
353 28.916 185
$
GENERATE BETWEEN 1 13 93 81
XDIRECTION 6 PARTS EQUAL
YDIRECTION 4 PARTS EQUAL
$
GENERATE BETWEEN 81 93 253 241
XDIRECTION 6 PARTS EQUAL
YDIRECTION 8 PARTS EQUAL
$
GENERATE BETWEEN 241 253 293 281
XDIRECTION 6 PARTS EQUAL
YDIRECTION 2 PARTS EQUAL
$
GENERATE BETWEEN 281 293 353 341
XDIRECTION 6 PARTS EQUAL
YDIRECTION 8 PARTS EQUAL
$
ADDITIONS
$
TYPE PLANE STRESS
GENERATE 6 ELEMENTS ID 1 1 F 1 2 T 3 2 T 23 2 T 21 2 T 2 2 -
    T 15 1 T 22 2 T 14 1
REPEAT 16 ID 6 F 20
$
$
STATUS SUPPORT 1 TO 13
$
$
$
$
```

Figure C1. Input data for mesh RBR6 (Continued)

```
$
ELEMENT PROPERTIES
1 TO 102 TYPE 'IP00' THICK 1.0
$
$
LOADING 1 'HYDROSTATIC LOADING USING EDGE LOADS'
$
ELEMENT LOADS
$
85  EDGE FORCE EDGE 4 GLOBAL VARIABLE VX  104.21  363.8  624.
79  EDGE FORCE EDGE 4 GLOBAL VARIABLE VX  624.     889.2 1154.4
73  EDGE FORCE EDGE 4 GLOBAL VARIABLE VX 1154.4  1419.6 1684.8
67  EDGE FORCE EDGE 4 GLOBAL VARIABLE VX 1684.8  2062.9 2441.4
61  EDGE FORCE EDGE 4 GLOBAL VARIABLE VX 2441.4  2819.9 3198.
55  EDGE FORCE EDGE 4 GLOBAL VARIABLE VX 3198.    3576.1 3954.6
49  EDGE FORCE EDGE 4 GLOBAL VARIABLE VX 3954.6  4333.1 4711.2
43  EDGE FORCE EDGE 4 GLOBAL VARIABLE VX 4711.2  5089.3 5467.8
37  EDGE FORCE EDGE 4 GLOBAL VARIABLE VX 5467.8  5846.1 6224.4
31  EDGE FORCE EDGE 4 GLOBAL VARIABLE VX 6224.4  6602.7 6981.
25  EDGE FORCE EDGE 4 GLOBAL VARIABLE VX 6981.    7359.3 7737.6
19  EDGE FORCE EDGE 4 GLOBAL VARIABLE VX 7737.6  8096.4 8455.2
13  EDGE FORCE EDGE 4 GLOBAL VARIABLE VX 8455.2  8814.   9172.8
7   EDGE FORCE EDGE 4 GLOBAL VARIABLE VX 9172.8  9531.6 9890.4
1   EDGE FORCE EDGE 4 GLOBAL VARIABLE VX 9890.4 10249.2 10608.0
$
$
LOADING 2 'SELF-WEIGHT USING BODY FORCE'
ELEMENT LOAD
1 TO 102 BODY FORCE GLOBAL BY -150.0
$
LOADING COMBINATION 3 '1 + 2' COMBINE 1 1.0 2 1.0
$
CONSTANTS
E 576000000.
POISSON 0.2
$
STIFFNESS ANALYSIS
$
LIST REACTIONS
$
LIST SUM REACTION
$
CALCULATE AVERAGE STRESSES
$
$
SAVE 'RBR6'
FINISH
```

Figure C1. (Concluded)

WATERWAYS EXPERIMENT STATION REPORTS PUBLISHED UNDER THE COMPUTER AIDED STRUCTURAL ENGINEERING (CASE) PROJECT

[illegible]	[illegible]	[illegible]
[illegible]	[illegible]	[illegible]
[illegible]	[illegible]	[illegible]
[illegible]	[illegible]	[illegible]
[illegible]	[illegible]	[illegible]
[illegible]	A Three-Dimensional Finite Element Data Edit Program	[illegible]
[illegible]	A Three-Dimensional Stability Analysis Design Program (3DSAD)	
	Report 1 General Geometry Module	[illegible]
	Report 3 General Analysis Module (CGAM)	[illegible]
	Report 4 Special-Purpose Modules for Dams (CDAMS)	Aug 1983
[illegible]	Basic User's Guide Computer Program for Design and Analysis of Inverted-T Retaining Walls and Floodwalls (TWDA)	Dec 1980
[illegible]	User's Reference Manual Computer Program for Design and Analysis of Inverted-T Retaining Walls and Floodwalls (TWDA)	Dec 1980
[illegible]	Documentation of Finite Element Analyses	
	Report 1 Longview Outlet Works Conduit	Dec 1980
	Report 2 Anchored Wall Monolith, Bay Springs Lock	Dec 1980
[illegible]	Basic Pile Group Behavior	Dec 1980
[illegible]	User's Guide Computer Program for Design and Analysis of Sheet Pile Walls by Classical Methods (CSHTWAL)	
	Report 1 Computational Processes	Feb 1981
	Report 2 Interactive Graphics Options	Mar 1981
[illegible]	Validation Report Computer Program for Design and Analysis of Inverted T Retaining Walls and Floodwalls (TWDA)	Feb 1981
[illegible]	User's Guide Computer Program for Design and Analysis of Cast-in-Place Tunnel Linings (NEWTUN)	Mar 1981
[illegible]	User's Guide Computer Program for Optimum Nonlinear Dynamic Design of Reinforced Concrete Slabs Under Blast Loading (CBARCS)	Mar 1981
[illegible]	User's Guide Computer Program for Design or Investigation of Orthogonal Culverts (CORTCUL)	Mar 1981
[illegible]	User's Guide Computer Program for Three-Dimensional Analysis of Building Systems (CTABS80)	Aug 1981
[illegible]	Theoretical Basis for CTABS80 A Computer Program for Three-Dimensional Analysis of Building Systems	Sep 1981
[illegible]	User's Guide Computer Program for Analysis of Beam-Column Structures with Nonlinear Supports (CBEAMC)	Jun 1982
[illegible]	User's Guide Computer Program for Bearing Capacity Analysis of Shallow Foundations (CBEAR)	Jun 1982

(Continued)

WATERWAYS EXPERIMENT STATION REPORTS PUBLISHED UNDER THE COMPUTER-AIDED STRUCTURAL ENGINEERING (CASE) PROJECT

(Concluded)

[illegible]	[illegible] (FRAME)	[illegible]
[illegible]	[illegible]	[illegible]
[illegible]	[illegible] Moment [illegible] Two-Dimensional [illegible] Analysis	[illegible]
[illegible]	[illegible]	[illegible]
[illegible]	Reference Manual: Computer Graphics Program for Generation of Engineering Geometry (SKETCH)	[illegible]
[illegible]	Case Study of Six Major General-Purpose Finite Element Programs	Oct [illegible]
[illegible]	User's Guide: Computer Program for Optimum Dynamic Design of Nonlinear Metal Plates Under Blast Loading (CSDOOR)	Jan 1984
[illegible]	User's Guide: Computer Program for Determining Induced Stresses and Consolidation Settlements (CSETT)	Aug 1984
[illegible]	Seepage Analysis of Confined Flow Problems by the Method of Fragments (CFRAG)	Sep 1984
[illegible]	User's Guide for Computer Program CGFAG, Concrete General Flexure Analysis with Graphics	Sep 1984
[illegible]	Computer-Aided Drafting and Design for Corps Structural Engineers	Oct 1984
Technical Report ATC-86-5	Decision Logic Table Formulation of ACI 318-77, Building Code Requirements for Reinforced Concrete for Automated Constraint Processing, Volumes I and II	Jun 1986
Report ITL-87-2	A Case Committee Study of Finite Element Analysis of Concrete Flat Slabs	Jan 1987
Report ITL-87-1	User's Guide: Computer Program for Two-Dimensional Analysis of U-Frame Structures (CUFRAM)	Apr 1987
Report ITL-87-2	User's Guide: For Concrete Strength Investigation and Design (CASTR) in Accordance with ACI 318-83	May 1987
Report ITL-87-6	Finite-Element Method Package for Solving Steady-State Seepage Problems	May 1987
Report ITL-87-3	User's Guide: A Three Dimensional Stability Analysis/Design Program (3DSAD), Report 1, Revision 1: General Geometry Module	Jun 1987
Report ITL-87-4	User's Guide: 2-D Frame Analysis Link Program (LINK2D)	Jun 1987
Report ITL-87-4	Finite Element Studies of a Horizontally Framed Miter Gate Report 1: Initial and Refined Finite Element Models (Phases A, B, and C), Volumes I and II Report 2: Simplified Frame Model (Phase D) Report 3: Alternate Configuration Miter Gate Finite Element Studies—Open Section Report 4: Alternate Configuration Miter Gate Finite Element Studies—Closed Sections	Aug 1987

(Continued)

WATERWAYS EXPERIMENT STATION REPORTS PUBLISHED UNDER THE COMPUTER-AIDED STRUCTURAL ENGINEERING (CASE) PROJECT

(Concluded)

	Title	Date
Technical Report ITL-87-4	Finite Element Studies of a Horizontally Framed Miter Gate Report 5: Alternate Configuration Miter Gate Finite Element Studies—Additional Closed Sections Report 6: Elastic Buckling of Girders in Horizontally Framed Miter Gates Report 7: Application and Summary	Aug 1987
Instruction Report GL-87-1	User's Guide: UTEXAS2 Slope-Stability Package; Volume I, User's Manual	Aug 1987
Instruction Report ITL-87-5	Sliding Stability of Concrete Structures (CSLIDE)	Oct 1987
Instruction Report ITL-87-6	Criteria Specifications for and Validation of a Computer Program for the Design or Investigation of Horizontally Framed Miter Gates (CMITER)	Dec 1987

END

DATE

FILMED

6-88

DTIC